Ministry for Primary Industries
Manatū Ahu Matua

The 2016 stock assessment of paua (*Haliotis iris*) for PAU 5D

New Zealand Fisheries Assessment Report 2017/33

C. Marsh
D. Fu

ISBN 978-1-77665-616-5 (online)
ISSN 1179-5352 (online)

June 2017

New Zealand Government

Growing and Protecting New Zealand

Requests for further copies should be directed to:

Publications Logistics Officer
Ministry for Primary Industries
PO Box 2526
WELLINGTON 6140

Email: brand@mpi.govt.nz
Telephone: 0800 00 83 33
Facsimile: 04-894 0300

This publication is also available on the Ministry for Primary Industries websites at:
http://www.mpi.govt.nz/news-and-resources/publications
http://fs.fish.govt.nz go to Document library/Research reports

TABLE OF CONTENTS

EXECUTIVE SUMMARY

Marsh, C.; Fu, D. (2017). The 2016 stock assessment of paua (*Haliotis iris*) for PAU 5D.

***New Zealand Fisheries Assessment Report 2017/33*. 48 p.**

This report summarises the stock assessment for paua (*Haliotis iris*) in PAU 5D (at the southern end of the New Zealand South Island), which included fishery data up to the 2015–16 fishing year. This report describes the model structure and output, including current and projected stock status. The data inputs are described in a separate Fisheries Assessment Report. The stock assessment was implemented as a length-based Bayesian estimation model implemented in AD Model Builder, with point estimates of parameters based on the mode of the joint posterior distribution, and uncertainty of model estimates investigated using the marginal posterior distributions generated from Markov chain-Monte Carlo simulation.

The data fitted in the assessment model were: (1) a standardised CPUE series derived from the early CELR data, (2) a standardised CPUE series derived from recent PCELR data, (3) commercial catch sampling length frequency series (CSLF), (4) tag-recapture length increment data, (5) maturity-at-length data. The research diver survey data were not used in this assessment because there was concern that the data were not a reliable index of abundance. Results from the previous assessment suggested the inclusion of the research diver survey indices had little influence on estimates of stock status.

The reference case model estimated that the unfished spawning stock biomass (B_0) was 2457 t (2270 – 2672 t), and the spawning stock population in 2016 (B_{2016}) was about 35% (28–43%) of B_0. The model projection made for three years assuming current catch levels, suggested that the spawning stock abundance will increase to about 38% (28–52%) of B_0 over the next three years. Two sensitivity runs were used in projections, the first sensitivity run doubled the observation error associated with the CPUE series, and the second assumed a hyper-stable relationship between CPUE and stock biomass using the shape parameter (h = 0.5). When the early CPUE series had double the observation error, the model estimated B_{2016} was about 32% (25–41%) of B_0. When the early CPUE series was assumed to have a hyper-stable relationship with biomass, the model estimated B_{2016} was 28% (22–37%) of B_0. All three models taken to projections concluded that the stock is very unlikely to fall below the soft and hard limit, and that the stock will increase under current catch levels.

1. INTRODUCTION

1.1 Overview

This report summarises the stock assessment for PAU 5D (at the southern end of the South Island, Figure 1) with the inclusion of data to the end of the 2015–16 fishing year. This report describes the model structure and output, including current and projected stock status. The input to the assessment are described elsewhere (Fu et al. 2017). The stock assessment was conducted with a length-based Bayesian estimation model first used in 1999 for PAU 5B (Breen et al. 2000a) with revisions made for subsequent assessments in PAU 5B (Breen et al. 2000b, Breen & Smith 2008a, Fu 2014a), PAU 4 (Breen & Kim 2004a), PAU 5A (Breen & Kim 2004b, Breen & Kim 2007, Fu & Mackenzie 2010a, b, Fu 2015a, 2015b), PAU 5D (Breen et al. 2000a, Breen & Kim 2007, Fu 2013), PAU 7 (Andrew et al. 2000, Breen et al. 2001, Breen & Kim 2003, 2005, McKenzie & Smith 2009a, Fu 2012, Fu 2016), and PAU 3 (Fu 2014b). PAU 5D was last assessed in 2011 (Fu 2013, Fu et al. 2013).

The six sets of data used in the assessment were: (1) a standardised CPUE series covering 1990–2001 based on CELR data (CPUE), (2) a standardised CPUE series covering 2002–2016 based on PCELR data (PCPUE), (3) a commercial catch sampling length frequency series (CSLF), (4) tag-recapture length increment data, (5) maturity-at-length data, (6) Catch history was an input to the model, encompassing commercial, recreational, customary, and illegal catch. These data inputs are described in detail by Fu et al. (2017).

Concerns have been raised about the veracity of the research diver survey methodology, and its usefulness in providing relative abundance indices (Cordue 2009, Haist 2010). In the most recent stock assessments of PAU 5A (Fu 2015a, b), PAU 5B (Fu 2014a), and PAU 5D (Fu 2013), the research diver survey indices (RDSI) and research diver survey length frequency (RDLF) data were not included in the base case model. A sensitivity analysis from the previous PAU 5D assessment (Fu 2013) suggested that both the survey abundance indices and length frequency data had very little influence on estimated stock status due to the large sampling uncertainties associated with these data. There have been no new research diver surveys since 2005, therefore they were only considered as sensitivity runs to the base case.

The assessment proceeded in several steps. First, the model was fitted to the data with parameters estimated at the mode of their joint posterior distribution (MPD). Next, from the resulting fit, Markov Chain-Monte Carlo (MCMC) simulations were used to obtain a large set of samples from the marginal posterior distribution. From this set of samples, forward projections were made, from which a set of agreed indicators were obtained. Sensitivity runs were explored by comparing MPD fits made with alternative model assumptions. MCMC simulations were also completed for a number of sensitivity runs.

This report fulfils part of Objective 1 "Undertake a stock assessment for PAU 5D, using a length-based Bayesian model", for Ministry for Primary Industries Project PAU201601.

1.2 Description of the fishery

The paua fishery was summarised by Schiel (1992), and in numerous previous assessment documents (e.g., Schiel 1989, McShane et al. 1994, 1996, Breen et al. 2000a, 2000b, 2001, Breen & Kim 2003, 2004a, 2004b, 2007, Breen & Smith 2008b, McKenzie & Smith 2009b, Fu et al. 2010, 2012, 2013, 2014a,b, 2015, 2016). A summary of the PAU 5D fishery up to the 2015–16 fishing year was presented by Fu et al. (2017).

2. MODEL

This section gives an overview of the model used for the stock assessment of PAU 5D in 2017; for furthur description see Breen et al. (2003). The model was developed for use in PAU 5B in 1999 and has been revised each year of subsequent assessments, in many cases echoing changes made to the rock lobster assessment model (Kim et al. 2004), which is a similar but more complex length-based Bayesian model.

2.1 Changes since the 2012 assessment model of PAU 5D

Three changes have been made to the stock assessment model since the last assessment of PAU 5D in 2012. One was to use a more flexible function form to describe the variance associated with the mean growth increment at length (See Section 2.2.7.2).

The second change was made so that the predicted CPUE was calculated after 50% of the fishing and natural mortality have occurred (previously the CPUE indices were fitted to the vulnerable biomass calculated after 50% of the catch was taken). This has been considered to be appropriate if the fishing occurs throughout a year (Schnute 1985). The change was recommended by the paua review workshop held in Wellington in March 2015 (Butterworth et al. 2015). Accordingly, mid-season number (and biomass) was calculated after half of the natural mortality and half of the fishing mortality was applied (See Section 2.2.7).

The third change was made to the likelihood function fitting the tag-recapture observations so that weights could be assigned to individual observations (see Section 2.2.8.1); this was also to follow the paua review workshop's recommendation that "the tagging data should be weighted by the relative contribution of average yield from the different areas so that the estimates could better reflect the growth rates from the more productive areas" (Butterworth et al. 2015).

2.2 Model description

The model partitioned the paua stock into a single sex population, with length classes from 70 mm to 170 mm, in groups of 2 mm (i.e., from 70 mm to less than 72 mm, 72 mm to less than 74 mm, etc.). The largest length bin was a plus group (170+ mm). The stock was assumed to be homogenous and reside in a single area. The partition accounted for numbers of paua by length class within an annual cycle, where movement between length classes was determined by estimated growth parameters. Paua entered the partition following a Beverton-Holt stock-recruitment relationship, and were removed by natural mortality and fishing mortality.

The model's annual cycle was based on the fishing year. References to "year" within this paper refer to the New Zealand fishing year (1 October to 30 September), and are labelled as year ending, i.e., the fishing year 1998–99 is referred to as "1999" throughout. Any references to calendar years are denoted specifically.

The models were run for the years 1965–2016. The model assumed one time step within an annual cycle. Catches were collated for 1974–2016, and were assumed to increase linearly between 1965 and 1973 from 0 to the 1974 catch level. Catches included commercial, recreational, customary, and illegal catch, and all catches occurred at the same time.

Recruitment was assumed to take place at the beginning of the annual cycle, and length at recruitment was defined by a uniform distribution with a range between 70 and 80 mm. Recruitment deviations (year class strengths) were assumed known and equal to 1 for the years up to 1980. This was ten years before the length data were available (loosely based on the approximate time taken for recruited paua to appear at the left hand side of the length distribution). The stock-recruitment relationship is unknown for paua, but is believed to be weak (Shepherd et al. 2001). A relationship may exist on small scales,

but may not be apparent when large-scale data are modelled (Breen et al. 2003), this follows the assumption of a single homogenous stock in the model. This assessment assumed a Beverton-Holt stock-recruitment relationship with a steepness (h) of 0.75 for the base case.

Maturity does not feature in the population partition. The model estimated proportion mature at each time step from length-at-maturity data. Growth and natural mortalities were also estimated within the model as time invariant parameters.

The models estimated two selectivities: the commercial fishing selectivity, and the Research Diver catch sample selectivity. Both selectivities had the option of following a logistic or double normal distribution (see 2.2.7.2).

The model was implemented in AD Model Builder™ (Otter Research Ltd., http://otter-rsch.com/admodel.htm) version 9.0.65, compiled with the MinGW 4.50 compiler.

2.2.1 Estimated parameters

Parameters estimated by the model were as follows. The parameter vector is referred to collectively as θ.

$\ln(R0)$ natural logarithm of average recruitment under equilibrium conditions

M instantaneous rate of natural mortality

g_1 expected annual growth increment at length L_1

g_2 expected annual growth increment at length L_2

ϕ CV of the expected growth increment

α parameter that defines the variance as a function of growth increment

β parameter that defines the variance as a function of growth increment

Δ_{max} maximum growth increment

l_{50}^{g} length at which the annual increment is half the maximum

l_{95}^{g} length at which the annual increment is 95% of the maximum

$l_{50}^{g} - l_{95}^{g}$ difference between l_{50}^{g} and l_{95}^{g}

q^{I} scalar between recruited biomass and CPUE

q^{I2} scalar between recruited biomass and PCPUE

L_{50} length at which maturity is 50%

$L_{95} - L_{50}$ interval between L_{50} and length at 95% selectivity

T_{50} length at RDLF selectivity is 50%

$T_{95} - T_{50}$ difference between T_{50} and length at 95% selectivity

D_{50} length at which commercial diver selectivity is 50%

$D_{95} - D_{50}$ difference between D_{50} and length at 95% selectivity

σ_R standard deviation for the right hand side of the double normal selectivity

σ_L standard deviation for the left hand side of the double normal selectivity

μ the mean for the double normal selectivity

D^{s} change in commercial diver selectivity for one unit change of MHS

$\tilde{\sigma}$ common component of error

h shape parameter defining non-linearity between CPUE and biomass.

$\boldsymbol{\varepsilon}$ vector of annual recruitment deviations, from 1980 to 2013

h steepness of the Beverton-Holt stock-recruitment relationship

2.2.2 Constants

l_k length of a paua at the midpoint of the k^{th} length class (l_k for class 1 is 71 mm, for class 2 is 73 mm and so on)

σ_{min} minimum standard deviation of the expected growth increment (assumed to be 1 mm)

σ_{obs} standard deviation of the observation error around the growth increment (assumed to be 0.25 mm)

MLS_t minimum legal size in year t (assumed to be 125 mm for all years)

$P_{k,t}$ a switch that describes whether abalone in the k^{th} length class in year t are above the minimum legal size (MLS) ($P_{k,t}$ = 1) or below ($P_{k,t}$ = 0)

a, b constants for the length-weight relation, taken from Schiel & Breen (1991) (2.592×10^{-8} and 3.322 respectively, converting length in millimetres to weight in kilograms)

w_k the weight of an abalone at length l_k

ϖ^I relative weight assigned to the CPUE dataset. This and the following relative weights were varied between runs to find a base case model run with balanced residuals

ϖ^{I2} relative weight assigned to the PCPUE dataset

ϖ^s relative weight assigned to CSLF dataset

ϖ^{mat} relative weight assigned to maturity-at-length data

ϖ^{tag} relative weight assigned to tag-recapture data

ϖ_j^{tag} relative weight assigned to tag-recapture observations that from area j

U^{max} exploitation rate above which a limiting function was invoked (0.80 for the base case)

μ_ε mean of the prior distribution for M

σ_M assumed standard deviation of the prior distribution for M

σ_ε assumed standard deviation of recruitment deviations in log space for years 1980–2012 (part of the prior for recruitment deviations)

n_ε number of recruitment deviations

L_1 length associated with g_1 (75 mm)

L_2 length associated with g_2 (120 mm)

D_t^a Change in Minimum Harvest Size (MHS) in year t, (exogenous variable associated with the change in commercial diver selectivity in year t)

2.2.3 Observations

C_t observed catch in year t

I_t standardised CPUE in year t

$I2_t$ standardised PCPUE in year t

σ_t^I standard deviation of the estimate of observed CPUE in year t, obtained from the standardisation model

cv_t^I CV of the estimate of observed CPUE in year t, obtained from the standardisation model

σ_t^{I2} standard deviation of the estimate of observed PCPUE in year t, obtained from the standardisation model

cv_t^{I2} CV of the estimate of observed PCPUE in year t, obtained from the standardisation model

$p_{k,t}^s$ observed proportion in the k^{th} length class in year t in CSLF

l_j initial length for the j^{th} tag-recapture record

d_j observed length increment of the j^{th} tag-recapture record

Δt_j time at liberty for the j^{th} tag-recapture record

P_k^{mat} observed proportion mature in the k^{th} length class in the maturity dataset

2.2.4 Derived variables

R0 average number of annual recruits under equilibrium conditions

$N_{k,t}$ number of paua in the k^{th} length class at the start of year *t*

$N_{k,t+0.5}$ number of paua in the k^{th} length class in the mid-season of year *t*

$R_{k,t}$ recruits to the model in the k^{th} length class in year *t*

g_k expected annual growth increment for paua in the k^{th} length class

σ^{g_k} standard deviation of the expected growth increment for paua in the k^{th} length class, used in calculating $\mathbf{G}$

$\mathbf{G}$ growth transition matrix

B_t spawning stock biomass at the beginning of year *t*

$B_{t+0.5}$ spawning stock biomass in the mid-season of year *t*

B_0 spawning stock biomass assuming population in an equilibrium state.

B_t^r biomass of paua above the MLS at the beginning of year *t*

$B_{t+0.5}^r$ biomass of paua above the MLS in the mid-season of year *t*

B_0^r equilibrium biomass of paua above the MLS assuming no fishing and average recruitment from the period in which recruitment deviations were estimated

B_t^v vulnerable (to commercial fishing) biomass of paua at the beginning of year *t*

U_t exploitation rate in year *t*

A_t the complement of exploitation rate

$SF_{k,t}$ finite rate of survival from fishing for paua in the k^{th} length class in year *t*

V_k^k relative selectivity of commercial divers for paua in the k^{th} length class

$\sigma_{k,t}^s$ error of the predicted proportion in the k^{th} length class in year *t* in CSLF data

n_t^s relative weight (effective sample size) of the CSLF data in year *t*

σ_j^d standard deviation of the predicted length increment for the j^{th} tag-recapture record

σ_j^{tag} total error predicted for the j^{th} tag-recapture record

σ_k^{mat} error of the proportion mature-at-length for the k^{th} length class

$-\ln(\boldsymbol{L})$ negative log-likelihood

f total function value

2.2.5 Predictions

$\hat{I}_t$ predicted CPUE in year *t*

$\hat{I2}_t$ predicted PCPUE in year *t*

$\hat{P}_{k,t}^r$ predicted proportion in the k^{th} length class in Research Diver LF

$\hat{P}_{k,t}^s$ predicted proportion in the k^{th} length class in year *t* in commercial catch sampling

$\hat{d}_j$ predicted length increment of the j^{th} tag-recapture record

$\hat{P}_k^{mat}$ predicted proportion mature in the k^{th} length class

2.2.6 Initial conditions

The initial population was assumed to be in equilibrium with zero fishing mortality and the base recruitment (R0). The model was run for 60 years with no fishing to obtain near-equilibrium in numbers-at-length. Recruitment was evenly divided among the first five length bins:

(1) $R_{k,t} = 0.2R0$ for $1 \le k \le 5$

(2) $R_{k,t} = 0$ for $k > 5$

A growth transition matrix was calculated inside the model from the estimated growth parameters. The base case used the exponential model and the expected annual growth increment for the k^{th} length class was:

(3) $\Delta l_k = g_1 \left(g_2 / g_1\right)^{(l_k - L_1)/(L_2 - L_1)}$

If the growth model was an inverse-logistic model, the expected annual growth increment for the k^{th} length class was:

(4) $\Delta l_k = \dfrac{\Delta_{\max}}{\left(1 + \exp\left(\ln(19)\left(\left(l_k - l^g_{50}\right)/\left(l^g_{95} - l^g_{50}\right)\right)\right)\right)}$

If the growth model was linear, the expected annual growth increment for the k^{th} length class was:

(5) $\Delta l_k = \left(\dfrac{L_2 g_1 - L_1 g_2}{g_1 - g_2} - l_k\right)\left[1 - \left(1 + \dfrac{g_{1-} g_2}{L_1 - L_2}\right)\right]$

The model used the AD Model Builder™ function *posfun*, with a dummy penalty, to ensure a positive expected increment at all lengths, using a smooth differentiable function.

All the models were examined and the exponential growth model was chosen for fitting the tag-recapture data in the base case of the PAU 5D assessment.

The standard deviation of g_k was assumed to be proportional to g_k with minimum σ_{MIN}:

(6) $\sigma^{g_k} = \left(g_k \phi - \sigma_{MIN}\right)\left(\dfrac{1}{\pi}\tan^{-1}\left(10^6\left(g_k \phi - \sigma_{MIN}\right)\right) + 0.5\right) + \sigma_{MIN}$

Or a more complex functional form between the growth increment and its standard deviation defined as:

(7) $\sigma^{g_k} = \left(\alpha\left(g_k\right)^{\beta} - \sigma_{MIN}\right)\left(\dfrac{1}{\pi}\tan^{-1}\left(10^6\left(\alpha\left(g_k\right)^{\beta} - \sigma_{MIN}\right)\right) + 0.5\right) + \sigma_{MIN}$

From the expected increment and standard deviation for each length class, the probability distribution of growth increments for a paua of length l_k was calculated from the normal distribution and translated into the vector of probabilities of transition from the k^{th} length bin to other length bins to form the growth transition matrix **G**. Zero and negative growth increments were permitted, i.e., the probability of staying in the same bin or moving to a smaller bin could be non-zero.

In the initialisation, the vector $\mathbf{N_t}$ of numbers-at-length was determined from numbers in the previous year, survival from natural mortality, the growth transition matrix **G,** and the vector of recruitment $\mathbf{R_t}$:

(8) $\mathbf{N_t} = \left(\mathbf{N_{t\text{-}1}}\, e^{-M}\right) \bullet \mathbf{G} + \mathbf{R_t}$

where the dot (•) denotes matrix multiplication.

2.2.7 Dynamics

2.2.7.1 Sequence of operations

After initialisation, the first model year was 1965 and the model was run through to 2015. In the first nine years the model was run with an assumed catch vector, because it was unrealistic to assume that the fishery was in a virgin state when the first catch data became available in 1974. The assumed catch vector increased linearly from zero to the 1974 catch. These years can be thought of as an additional part of the initialisation, but they use the dynamics described in this section.
Model dynamics were sequenced as follows.

- Numbers at the beginning of year *t*-1 were subjected to fishing, followed by natural mortality, then growth, to produce the numbers at the beginning of year *t*.
- Recruitment was added to the numbers at the beginning of year *t*.
- Biomass available to the fishery was calculated and, with catch, was used to calculate the exploitation rate, which was constrained if necessary.
- Half the exploitation rate and half natural mortality were applied to obtain mid-season numbers, from which the predicted abundance indices and proportions-at-length were calculated. Mid-season numbers were not used further.

2.2.7.2 Main dynamics

For each year *t*, the model calculated the start-of-the-year biomass available to the commercial fishery. Biomass available to the commercial fishery was:

(9) $$B_t^v = \sum_k N_{k,t} V_k^s w_k$$

(10) $$V_k^{t,s} = \frac{1}{1+19^{-\left(\left(l_k - D_{50}\right)/D_{95-50}\right)}}$$ for $t < 2006$ assuming logistic selectivity

(11) $$V_k^{t,s} = \frac{1}{1+19^{-\left(\left(l_k - D_{50} - D_t^a D^s\right)/D_{95-50}\right)}}$$ for $t \geq 2006$ assuming logistic selectivity

(12) $$V_k^{t,s} = \begin{cases} 2^{-\left[\frac{(l_k-\mu)}{\sigma_L}\right]^2} & (l_k \leq \mu) \\ 2^{-\left[\frac{(l_k-\mu)}{\sigma_R}\right]^2} & (l_k > \mu) \end{cases}$$ for $t < 2006$ assuming double normal selectivity

(13) $$V_k^{t,s} = \begin{cases} 2^{-\left[\frac{(l_k-\mu-D_t^a D^s)}{\sigma_L}\right]^2} & (l_k \leq \mu) \\ 2^{-\left[\frac{(l_k-\mu-D_t^a D^s)}{\sigma_R}\right]^2} & (l_k > \mu) \end{cases}$$ for $t \geq 2006$ assuming double normal selectivity

This model has the option of two selectivities for the fishery; either the logistic (Equations 10 and 11) or the double normal (Equations 12 and 13). The observed catch was then used to calculate the exploitation rate, constrained for all values above U^{max} with the *posfun* function of AD Model Builder™. If the ratio of catch to available biomass exceeded U^{max}, then exploitation rate was constrained and a penalty was added to the total negative log-likelihood function. Let minimum survival rate A_{min} be 1-U^{max} and survival rate A_t be 1-U_t:

(14) $$A_t = 1 - \frac{C_t}{B_t^v}$$ for $\frac{C_t}{B_t^v} \leq U^{\max}$

(15) $$A_t = 0.5A_{\min}\left[1+\left(3-\frac{2\left(1-\frac{C_t}{B_t^v}\right)^{-1}}{A_{\min}}\right)\right] \quad \text{for} \quad \frac{C_t}{B_t^v} > U^{\max}$$

The penalty invoked when the exploitation rate exceeded U^{max} was:

(16) $$10000000\left(A_{min}-\left(1-\frac{C_t}{B_t^r}\right)\right)^2$$

This prevented the model from exploring parameter combinations that gave unrealistically high exploitation rates. Survival from fishing was calculated as:

(17) $$SF_{k,t} = 1-(1-A_t)P_{k,t}$$

or

(18) $$SF_{k,t} = 1-(1-A_t)V_k^s$$

The vector of numbers-at-length in year t was calculated from numbers in the previous year:

(19) $$\mathbf{N_t} = \left(\left(\mathbf{SF_{t\text{-}1}} \otimes \mathbf{N_{t\text{-}1}}\right)\mathrm{e}^{-M}\right) \bullet \mathbf{G} + \mathbf{R_t}$$

where $\otimes$ denotes the element-by-element vector product. The vector of recruitment, $\mathbf{R_t}$, was determined from *R0*, estimated recruitment deviations, and the stock-recruitment relationship:

(20) $$R_{k,t} = 0.2R0e^{\left(\varepsilon_t - 0.5\sigma_t^2\right)}\frac{B_{t-1+0.5}}{B_0}\Big/\left(1-\frac{5H-1}{4H}\left(1-\frac{B_{t-1+0.5}}{B_0}\right)\right) \quad \text{for } 1 \le k \le 5$$

(21) $$R_{k,t} = 0 \quad \text{for } k > 5$$

The recruitment deviation parameters ε_t were estimated for all years from 1980. The recruitment deviations were constrained to have a mean of 1 in arithmetic space.

The model predicted CPUE in year t from mid-season recruited biomass, the scaling coefficient, and the shape parameter:

(22) $$\hat{I}_t = q^I(B_{t+0.5}^v)^h$$

Available biomass $B_{t+0.5}^v$ was the mid-season vulnerable biomass after half the catch had been removed and half natural mortality applied (because the catch occurred throughout the fishing year). It was calculated as in equation 9, but using the mid-year numbers, $N_{k,t+0.5}$:

(23) $$N_{t+0.5} = N_t \exp(-0.5M)\left(1-\frac{(1-A_t)}{2}V_t^s\right)$$

Similarly,

(24) $$\hat{I}2_t = q^{I2}(B_{t+0.5}^v)^h$$

The same shape parameter h was used for both the early and recent CPUE series.

The Research Diver LF selectivity V_k^r was calculated from:

$$V_k^F = \frac{1}{1+19^{-\left(\left(l_k - T_{50}\right)/T_{95-50}\right)}} \quad (25)$$

The model predicted proportions-at-length for the CSLF from numbers in each length class for lengths greater than 116 mm:

$$\hat{P}_{k,t}^S = \frac{N_{k,t+0.5}V_{k,t}^S}{\sum_{k=23}^{51} N_{k,t+0.5}V_{k,t}^S} \quad (26)$$

Predicted proportions-at-length for RDLF were similar:

$$\hat{P}_{k,t}^F = \frac{N_{k,t+0.5}V_{k,t}^F}{\sum_{k=25}^{51} N_{k,t+0.5}V_{k,t}^F} \quad (27)$$

The predicted increment for the j^{th} tag-recapture record, using the inverse-logistic model, was:

$$\hat{d}_j = \frac{\Delta_{max}}{\left(1+exp\left(\ln(19)\left(l_j - l_{50}^g\right)/\left(l_{95}^g - l_{50}^g\right)\right)\right)} \quad (28)$$

where Δt_j is in years. For the exponential model the expected increment was

$$\hat{d}_j = \Delta t_j g_\alpha \left(g_\beta / g_\alpha\right)^{\left(L_j - \alpha\right)/(\beta - \alpha)} \quad (29)$$

The error around an expected increment was:

$$\sigma_j^d = \left(\alpha\left(\hat{d}_j\right)^\beta - \sigma_{min}\right)\left(\frac{1}{\pi}tan^{-1}\left(10^6\left(\alpha\left(\hat{d}_j\right)^\beta - \sigma_{min}\right)\right) + 0.5\right) + \sigma_{min} \quad (30)$$

Predicted maturity-at-length was:

$$\hat{p}_k^{mat} = \frac{1}{1+19^{-\left(\left(l_k - L_{50}\right)/L_{95-50}\right)}} \quad (31)$$

2.2.8 Fitting

2.2.8.1 Likelihoods

The distribution of CPUE is assumed to be normal-log and the negative log-likelihood is:

$$-\ln(\boldsymbol{L})\left(\hat{I}_t \middle| \theta\right) = \frac{\left(\ln(I_t) - \ln(\hat{I}_t)\right)}{2\left(\sigma_t^I \tilde{\sigma}/\varpi^I\right)} + \ln\left(\sigma_t^I \tilde{\sigma}/\varpi^I\right) + 0.5\ln(2\pi) \quad (32)$$

Where

$$\sigma_t^I = \sqrt{\log\left(\left(cv_t^I\right)^2 + 1\right)} \quad (33)$$

and similarly for PCPUE:

$$-\ln(\boldsymbol{L})\left(\hat{I2}_t \middle| \theta\right) = \frac{\left(\ln(I_{2t}) - \ln(\hat{I2}_t)\right)}{2\left(\sigma_t^{I2} \tilde{\sigma}/\varpi^{I2}\right)} + \ln\left(\sigma_t^{I2} \tilde{\sigma}/\varpi^{I2}\right) + 0.5\ln(2\pi) \quad (34)$$

Where

(35) $$\sigma_t^{I2} = \sqrt{\log((cv_t^{I2})^2 + 1)}$$

The proportions-at-length from CSLF data are assumed to follow a multinomial distribution, with a standard deviation that depends on the effective sample size (see Section 2.2.9.3) and the weight assigned to the data:

(36) $$\sigma_{k,t}^{s} = \frac{\widetilde{\sigma}}{\varpi^{s} n_t^{s}}$$

The negative log-likelihood is:

(37) $$-\ln(L)\left(\hat{P}_{k,t}^{s}|\theta\right) = \frac{P_{k,t}^{s}}{\sigma_{k,t}^{s}}\left(ln\left(P_{k,t}^{s} + 0.01\right) - \ln\left(\hat{P}_{k,t}^{s} + 0.01\right)\right)$$

Errors in the tag-recapture dataset were also assumed to be normal. For the j^{th} record, the total error is a function of the predicted standard deviation (equation 38), observation error, and weight assigned to the data:

(38) $$\sigma_j^{tag} = \tilde{\sigma}/\varpi^{tag}\sqrt{\sigma_{obs}^2 + (\sigma_j^d)^2}$$

The negative log-likelihood for an observation is:

(39) $$-\ln(\boldsymbol{L})\left(\hat{d}_j|\theta\right) = \varpi_g^{tag}\left(\frac{(d_j - \hat{d}_j)^2}{2\left(\sigma_j^{tag}\right)^2} + \ln\left(\sigma_j^{tag}\right)^2 + 0.5\ln(2\pi)\right)$$

where ω_g^{tag} is a weighing factor calculated as

(40) $$\omega_g^{tag} = p_g \frac{\sum_g n_g}{n_g}$$

where p_g is the proportion of catch from area g (where the observation is made), and n_g is the number of tag-recapture observations from area g. This allows the likelihood to be influenced by the catch proportion of each area, but not the size of observations. ω_g^{tag} can be fixed at 1 if the likelihood is not to be weighted.

The proportion mature-at-length was assumed to be normally distributed, with standard deviation analogous to proportions-at-length:

(41) $$\sigma_k^{mat} = \frac{\tilde{\sigma}}{\varpi^{mat}\sqrt{P_k^{mat}+0.1}}$$

The negative log-likelihood is:

(42) $$-\ln(\mathbf{L})\left(\hat{p}_k^{mat}\,|\,\theta\right) = \frac{\left(p_k^{mat} - \hat{p}_k^{mat}\right)^2}{2\left(\sigma_k^{mat}\right)^2} + \ln\left(\sigma_k^{mat}\right) + 0.5\ln\left(2\pi\right)$$

2.2.8.2 Normalised residuals

These are calculated as the residual divided by the relevant σ term used in the likelihood. For CPUE, the normalised residual is

(43) $$\frac{\ln(I_t) - \ln(\hat{I}_t)}{\left(\sigma_t^I \tilde{\sigma}/\varpi^I\right)}$$

and similarly for PCPUE. For the CSLF proportions-at-length, the residual is:

(44) $\frac{p^s_{k,t}-\hat{p}^s_{k,t}}{\sigma^s_{k,t}}$

For tag-recapture data, the residual is:

(45) $\frac{d_j-\hat{d}_j}{\sigma_j^{tag}}$

and for the maturity-at-length data the residual is:

(46) $\frac{p_k^{mat}-\hat{p}_k^{mat}}{\sigma_k^{mat}}$

2.2.8.3 Dataset weights

Proportions at length (CSLF and RDLF) were included in the model with a multinomial likelihood. The length frequencies for individual years were assigned relative weights (effective sample size), based on a sample size that represented the best least squares fit of log(cv_i)~log(P_i), where cv_i was the bootstrap CV for the ith proportion, P_i. (See Figure A6, Appendix A, for a plot of this relationship). The weights for individual years (n_t^s for CSLF and n_t^F for RDLF) were multiplied by the weight assigned to the dataset (ϖ^s for CSLF and ϖ^F for RDLF) to obtain the model weights for the observations. We used the weighting scheme following Francis (2011) for the base case model, where the weight for the CSLF dataset was determined as

(47) $\varpi^s = 1/\mathrm{var}_t\left[\left(\overline{O}_t^s - \overline{E}_t^s\right)/\left(v_t^s/n_t^s\right)^{0.5}\right]$ (Method TA1.8, table A1 in Francis 2011)

Where

(48) $\overline{O}_t^s = \sum_k p_{k,t}^s l_k$

(49) $\overline{E}_t^s = \sum_k \hat{p}_{k,t}^s l_k$

(50) $V_t^s = \sum_k l_k^2 \hat{P}_{k,t}^s - (\bar{E}_t^s)^2$

The TA1.8 method allows for the possibility of substantial correlations within a dataset, and generally produces relatively small sample sizes, thus down-weighting the composition data (Francis 2011). The actual and estimated sample sizes for the commercial catch at length using the two methods are given in Table 1.

The relative abundance indices (CPUE and PCPUE) were included in the model with a lognormal likelihood. The weights for individual years were determined by the CV calculated in the standardisation and were then scaled by the weight assigned to the dataset to obtain the model weights for the observations. In previous assessments, the weight of the dataset was determined iteratively so that the standard deviation of the normalised residuals was close to one. In this assessment, we used a weighting scheme recommended by Francis (2011), with a small modification recommended by the review workshop (Butterworth et al. 2015). With this approach, a series of loess lines of various degrees of smoothing were fitted to the abundance indices (this was carried out outside the assessment model), and the CV was calculated using the residuals from the loess line which was considered to have the "appropriate" smoothness. This CV was then adjusted for the degrees of freedom associated with the smoothing:

(51) $\widetilde{cv} = cv\left(\frac{n}{n-d}\right)$

Where CV was calculated using the residuals, n is the number of indices, d is degree of freedom, and $\widetilde{cv}$ was the adjusted value. The adjusted CV was applied to all years in the time series and remained constant in the stock assessment model. The choice of the "appropriate" fit was based on visual

examination of the loess lines. This is equivalent to saying that we expected the stock assessment model to fit these data as well as the smoother.

For the early CPUE (1990–2001), the residuals from the loess line which had the "appropriate" smoothness (d=5) had an adjusted CV of 0.1 (Figure A7–left, Appendix A); for the recent CPUE (2002–2015), a CV of 0.08 was considered to be appropriate (d=5, Figure A2–right, Appendix A). The CVs of the CPUE observations in the assessment model were fixed at those values (except for sensitivity run 0.1e in which alterative values were assumed).

2.2.8.4 Priors and bounds

Bayesian priors were established for all estimated parameters (Table 2). Most had uniform (uninformed) distributions with upper and lower bounds set arbitrarily wide so as not to constrain the estimation. The prior probability density for M was a normal-log distribution with mean μ_M and standard deviation σ_M. The contribution to the objective function of estimated $M = x$ is:

$$-\ln(\mathbf{L})(x \mid \mu_M, \sigma_M) = \frac{\left(\ln(M) - \ln(\mu_M)\right)^2}{2\sigma_M{}^2} + \ln\left(\sigma_M \sqrt{2\pi}\right) \quad (52)$$

The prior probability density for the vector of estimated recruitment deviations ε, was assumed to be normal with a mean of zero and a standard deviation of 0.4. The contribution to the objective function for the whole vector is:

$$-\ln(\mathbf{L})(\varepsilon \mid \mu_\varepsilon, \sigma_\varepsilon) = \frac{\sum_{i=1}^{n_\varepsilon} (\varepsilon_i)^2}{2\sigma_\varepsilon{}^2} + \ln(\sigma_\varepsilon) + 0.5\ln(2\pi). \quad (53)$$

2.2.8.5 Penalty

A penalty was applied to exploitation rates higher than the assumed maximum (equation 13). The penalty was added to the objective function after being multiplied by an arbitrary weight (1000000).

AD Model Builder™ also has internal penalties that keep estimated parameters within their specified bounds, but these should have no effect on the final outcome, because choice of a base case excluded the situations where parameters were estimated at or near a bound.

2.2.9 Fishery indicators

The assessment calculates the following quantities from their posterior distributions of the model's mid-season spawning and recruited biomass for 2015 ($B_{current}$ and $B^r_{current}$) and for the projection period (B_{proj} and B^r_{proj}).

Simulations were carried out to calculate deterministic MSY, the maximum constant annual catch that can be sustained under deterministic recruitment. A single simulation run was done by starting from an unfished equilibrium state, and running under a constant exploitation rate until the catch and spawning stock biomass stabilised. For each simulation run with exploitation rate U, the equilibrium total annual catch and spawning stock biomass were calculated. The exploitation rate U that maximized the annual catch was U_{msy}. The corresponding catch was MSY, and the corresponding SSB was B_{msy}. Together with B_0, B_{msy}, $U_{current}$, $U_{\%40B0}$ and U_{msy} the current and projected stock status was reported in relation to the following indicators:

$\%B_0$	current and projected spawning biomass as a percent of B_0,
$\%B_{msy}$	current and projected spawning biomass as a percent of B_{msy}
$Pr(>B_{current})$	Probability that current and projected spawning biomass is greater than $B_{current}$
$Pr(>B_{msy})$	Probability that current and projected spawning biomass is greater than B_{msy}
$\%B_0^r$	current and projected recruited biomass as a percent of B_0^r
$\%B_{msy}^r$	current and projected recruited biomass as a percent of B_{msy}^r
$Pr(>B_{msy}^r)$	Probability that current and projected recruit-sized biomass is greater than B_{msy}^r
$Pr(>B_{current}^r)$	Probability that projected recruit-sized biomass is greater than $B_{current}^r$
$Pr(B_{proj} > 40\%B_0)$	Probability that current and projected spawning biomass is greater than 40% B_0
$Pr(B_{proj} < 20\%B_0)$	Probability that current and projected spawning biomass is less than 20% B_0
$Pr(B_{proj} < 10\%B_0)$	Probability that current and projected spawning biomass is less than 10% B_0
$Pr(U_{proj} > U_{40\%B0})$	Probability that current and projected exploitation rate is greater than $U_{40\%B0}$

2.2.10 Markov chain-Monte Carlo (MCMC) procedures

AD Model Builder™ uses the Metropolis-Hastings algorithm to conduct MCMC. The step size was based on the standard errors of the parameters and their covariance relationships, estimated from the Hessian matrix.

For the MCMCs in this assessment, single long chains were run, starting at the MPD estimate. The base case was 5 million simulations, from which every 5000th sample was saved. The value of $\tilde{\sigma}$ was fixed to that used in the MPD run because it may be inappropriate to let a variance component change during the MCMC.

2.2.11 Development of base case and sensitivity model runs

The starting point for this year's base case model configuration was the base case from the last accepted assessment for PAU 5D (Fu 2013). The first step in developing an updated base model was to view the effects of these model changes (see Section 2.1) by comparing the outputs between the 2012 assessment model and the current assessment model with the same data used in the 2012 assessment. The models gave a similar output (Figure 2); this was also found when applying the revised model in the PAU 7 stock assessment (Fu 2016).

The Shellfish Working Group (SFWG) then requested an ensemble of initial model runs to be conducted. The initial models investigated aspects of model configurations such as data weighting methods, choice of growth model, and the inclusion of alternative CPUE indices and catch histories. The configurations of the initial model runs are summarised in Table A1. The results of the initial model runs are briefly summarised in Section 3.1.

After reviewing the diagnostics and outputs from the preliminary model runs (Section 3.1), the SFWG requested one base case model run, Model 0.0, which assumed the exponential growth model. The base

case model was configured such that (a) predicted CPUE was calculated after half of the natural and fishing mortality has occurred; (b) the Francis (2011) method was used to determine the weight of CSLF and CPUE; (c) tag-recapture observations were not weighted by the catch ($\omega_g^{tag} = 1$); (d) the natural mortality *M* was estimated with a lognormal prior with $\mu_M = 0.1$ and CV_M of 0.1; (e) the CPUE shape parameter was fixed at 1, thereby assuming a linear relationship between CPUE and abundance.

The SFWG also requested a subset of sensitivity runs from the initial model runs presented, these were: doubling the CV on both CPUE series (model 0.0e), using an alternative mean for the lognormal prior on M where $\mu_M = 0.15$ (model 0.0b), fixing the shape parameter (h) on both CPUE series at 0.5 (model 0.0h) and modelling growth using the inverse-logistic model (model 0.1). A description of the base case and sensitivity models is given in Table 4. Results from Maximum Posterior Densities (MPD) estimates for model parameters, fits and reference points are summarised in Table 5.

3. RESULTS

3.1 Preliminary model runs

Initial model runs considered a large range of model configurations, which generated candidate models for the base case and sensitivities runs. Key conclusions drawn from the initial diagnostics are summarised below.

- Assuming that half of the fishing and natural mortality had occurred when calculating CPUE fits, appeared to have little effect on the model derived quantities, but resulted in slightly higher equilibrium biomass estimate (Figure 2).
- Weighting tag-recapture observations by the catch had little effect when growth was parameterised with the inverse-logistic growth model (Figure A1 right panel). For the exponential growth model weighting tagging data by catch generated slightly lower estimates of mean growth (Figure A1 left panel), which resulted in higher estimates of B_0, $B_{current}$ and % B_0 (see Figure 11).
- Estimating the CPUE shape parameter (h) with a uniform prior with bounds 0.3 – 2 which was applied to both CPUE series. The estimate of h hit the lower bound (0.3) suggesting a hyper-stable relationship. This was considered by the SFWG to be a severe hyper-stable relationship, and the SFWG expressed concern with such an extreme non-linear relationship.
- Applying a double normal selectivity for fishery vulnerability was explored as an alternative to the logistic. The RDLF's from the early 90s had a small mode of large fish that wasn't observed in the CSLF (Figure A2). The double normal was used to investigate the assumption of having a cryptic biomass that wasn't available to the fishery. The parameter controlling the right hand limb of the selectivity (σ_R) was estimated to be small, implying a large cryptic biomass. The SFWG considered a large cryptic biomass to be implausible. When fixing the right hand standard deviation at arbitrary values there was little difference between the double normal and logistic selectivity fits.
- Including the RDLF for 1992 yielded a slightly higher % B_0 (36%) relative to the base case (33%) with slightly higher estimates of B_0 and % $B_{current}$.
- Observation error associated with CPUE series was arbitrarily doubled for both CPUE series to explore the effects of a more uncertain CPUE series. This caused the model to have a poorer

fit to the first CPUE series (Figure A3). This changed model parameters and outcomes but had little effect on fits to other data sets.

- The exponential and inverse-logistic growth model were both explored. The exponential growth model resulted in a better fit to the CSLF data (Figure A5), but didn't fit the tag recapture data as well at both limits of the data (Figure A4).
- Alternative priors on natural mortality (*M*) were also considered. One large uncertainty in this model is the value of M . When the mean of the prior was increased from 0.1 to 0.15, the estimate of *M* moved in the same direction as the prior. The estimate of *M* when $\mu_M = 0.1$ was 0.14, when the $\mu_M = 0.15$ the estimate was 0.18. This suggested that the estimate of M was sensitive to the choice of the prior, which had been observed in previous assessments.
- Other sensitivity runs included removing tag recapture observations less than 90 mm, combining both CPUE series, and using alternative recreational catch histories, but all had negligible effect on the model outputs.

3.2 MPD base case and sensitivity runs

MPD estimates of objective function values (negative log-likelihood), parameters, and indicators for the base case and sensitivity runs are summarised in Table 5. The base case model predicted the main trends observed in both CPUE series well, and the most fits were within the confidence bounds of the observed values, with the exception of the first year (1990) of the series (Figure 3). The base case model struggled to fit observations that deviated away from the overall trend, for example years 1999, 2006 and 2011 (Figure 3). The standardised residuals showed no apparent departure to the model's assumption of normality (Figure 4), with the exception of the first year which fell outside the 95% confidence intervals.

Commercial catch length frequencies were fitted well for most years (Figure 5). The mean length of CSLF had been increasing between 2005 and 2013, with the last two years (2014 and 2015) decreasing (Figure 6–left panel). The standardised residuals of the fits to CSLF revealed that, in general, the model predicted slightly higher CSLF for the smaller sized fish (positive residuals) and slightly under predicted the larger sized fish (Figure 6–right). Estimated logistic selectivity was very close to knife-edge around the MLS, with a small increase in 2015 (Table 5, Figure 7). Fits to maturity data appeared adequate (Figure 7). The growth model over-estimated growth rates for smaller and larger fish, but did fit the majority of the tag data well (Figure 8). The slight misfits in the tails of the tag recapture data for the base case was a compromise that was chosen to obtain a better fit to the CSLF data when compared to the alternative inverse-logistic growth model (Figures A4 and A5).

Sensitivity runs that were selected by the SFWG from the initial model runs tested components of the model that had the most uncertainty attributed to them. The SFWG also requested sensitivity runs based on plausibility and that covered the range of expected uncertainty in current stock status. These components were; exponential vs inverse-logistic growth model, the quantity of observation error associated with the CPUE series, relationship between CPUE and true abundance and priors on natural mortality (M). These runs are summarised in Table 4. The fits between run 0.0b and the base case were very similar for all datasets. The current status of the stock from run 0.0b was estimated to be 40% B_0.

The CPUE shape parameter (*h*) was fixed to be 0.5 in sensitivity run 0.0h, implying a hyper-stable relationship between CPUE and biomass. In the initial runs, *h* was estimated at 0.3, but the SFWG considered this to be too extreme, and requested a sensitivity run with *h* of 0.5; this gave the lowest current stock status of all runs, with a current biomass at 22% B_0. This sensitivity run was considered plausible, because paua are susceptible to serial depletion (Abraham & Neubauer 2015), which can violate the assumption of linearity between CPUE and biomass. However, it was also acknowledged that for a fully developed fishery the assumption of linearity may be reasonable (Breen & Kim 2003).

The value of 0.5 was chosen based on a finfish study which considered values between 0.5 and 2.0 (Dunn et al. 2000).

Run 0.0e increased the CV's associated with both CPUE series; an arbitrarily choice was made to double the CV's so that CPUE CV = 0.2 and CPUE2 CV = 0.16. Run 0.0e didn't fit the trends of the early series as well as the base case, but did capture most of the trends on the second series (CPUE2) (Figure 9). The fits to the other data sets were similar to the base case. This sensitivity run was considered plausible because of SFWG concerns around how reliable the CPUE series were for tracking biomass.

The final sensitivity run (0.1) investigated the assumption of using the inverse-logistic growth model instead of the exponential growth model. The inverse-logistic growth model provided a better fit to the tag recapture data (Figure A4) but predicted larger fish in some years that generated a misfit in the CSLF data (Figure 10).

These chosen sensitivity runs represented the major concerns around structural assessment uncertainties, and gave current stock status of 22% –40% B_0. The relative SSB trajectories are shown in Figure 11.

3.3 MCMC results

The SFWG requested that model runs 0.0, 0.0b, 0.0e, 0.0h, and 0.1 be estimated by MCMC, to derive the posterior distributions of estimated parameters and biomass indicators.

All MCMC chains were diagnosed for convergence by assessing trace plots of the objective function and key parameters. The traces of key indicators (B_0 and $B_{current}$) across most chains showed no evidence of non-convergence, except for posterior samples from model 0.1 which exhibited instability (Figure 12).

3.3.1 Marginal posterior distributions and the Bayesian fit

For the base case and across the sensitivity runs, the estimated recent recruitment was below average from 2006 (Figure 13 right panel). The estimated exploitation rate was, on average, declining since 2003, then between 2011 and 2014 there was a slight increase in exploitation, followed by a decrease in 2015 and 2016 (Figure 13 left panel). The exploitation rate in 2016 was estimated to be 0.19 (95% CI 0.14–0.25). The decrease in exploitation rate in 2015 and 2016 followed the voluntary industry shelving of 30% of the TACC in those years.

SSB was estimated to have been decreasing from the beginning of exploitation (1965) until 2002, after which it remained relatively constant at 30–35% (Figure 14 left panel). Changes in stock size in response to fishing pressure over time are shown in Figure 15. The model indicated an early phase of the fishery when the exploitation rates were below $U_{40\%B0}$ and the SSBs were above 40% , then a development phase when the exploitation rates increased and the SSB decreased. The current exploitation rate was estimated to be around the target level of $U_{40\%B0}$ with the current spawning stock biomass just below 40% B_0.

Marginal posteriors were plotted for important productivity parameters natural mortality (M) and R_0, for comparison between sensitivity runs (Figure 16). There was a range of values estimated across the sensitivity and base case runs with runs. M was estimated to be above the base case for runs MCMC 0.0b and 0.1 and below the base case for runs MCMC 0.0e and 0.0h. For the parameter R_0, only run MCMC 0.0b estimated a higher value than the base case model.

Comparisons of marginal posteriors for $B_{current}$ are shown between the base case and sensitivities in Figure 17. The base case had the highest $B_{current}$ of 35% (95% CI 28% – 45%) and 0.0h had the lowest current status of 28% (95% CI 22%–37%). Estimates of biomass trajectories for all model runs are

shown in Figure 18. The median of current stock status was below 40% of B_0 but above 20% of B_0 for runs 0.0, 0.0e, and 0.0h, and was above 40% for runs 0.1, and 0.0b.

The SFWG considered three runs to be representative of the uncertainty in the assessment; these were 0.0 (base case), 0.0e, and 0.0h. The model runs had similar fits to the CPUE, with the most noticeable discrepancy being the greater variation produced by MCMC 0.0e (which was expected given it had double the uncertainty attributed to those observations) (Figure 19). All runs fitted the mean CSLF data similarly, tracking the general trend (Figure 20). In the years 2014 and 2015, the observed mean CSLF diverged from the previous increasing trend, which all three model runs struggled to fit, and on average they all estimated a higher mean CSLF. The model run fits were accepted by the SFWG, and the MCMC outputs used to assess future catch scenarios on the stock.

3.3.2 Projections

Three-year projections (2017–2019) were carried out for three model runs (0.0, 0.0e, and 0.0h).

In all projections, future recruitment deviations were resampled with equal probability from the MCMC sample estimates between 2002 and 2012. Future removals of fish from all sources (commercial, recreational, illegal and customary) were set to be the same in all future years. Future catches were the TACC reduced by 0% (current), 20%, 30% and 50%, but keeping recreational (10 t), illegal (10 t) and customary (2 t) the same. A sensitivity run changing the recreational catch to 20 t and having a 50% TACC reduction was also completed (labelled *50% reduction in Figure B1).

The projections for the base case model indicated that, with the assumed catch scenarios, the SSB was likely to remain flat or increase over the next three years (Figure top right); this trend was similar for all three model runs (Figure).

Under current catch levels the probability of the stock being above the target level of 40% B_0 for the base case increased from 14% in 2016 to 40% by 2019. For run MCMC 0.0e the same probability increased from 7% in 2016 to 23% in 2019, and for run 0.0h this probability increased from 2% in 2016 to 12% in 2019. In all model runs and catch scenarios it was very unlikely that the stock status would fall below the soft limit (Tables B1-B14, Appendix B).

4. DISCUSSION

The base case model suggested that the current spawning stock population ($B_{current}$) was 35% (95% CI 29–43%) B_0, and recruit-sized stock abundance ($B^r_{current}$) was 26% (95% CI 20–34%) of the initial recruit-sized state (B^r_r). The base case model suggested that the current stock status was very unlikely to fall below the soft limit. The projections suggested that biomass was likely to remain constant if the future catch were to be at the TACC, and increase if future catches were at current catch levels or below. This was the conclusion across all sensitivity runs.

The model presented here, whilst fairly representative of most data, also showed some lack of fit, and does contain structural uncertainties. The apparent decline of mean length in the commercial catch in 2014 and 2015 across the stock areas potentially indicated a decline in abundance. The model estimated an increase in abundance in 2014 and 2015, which was in agreement in the trend in recent CPUE which is suggestive of data conflict. CPUE can provide information on changes in relative abundance. However, CPUE is generally considered to be a poor index of stock abundance for paua, due to divers' ability to maintain catch rates by moving from area to area despite a decreasing biomass (hyperstability). Breen & Kim (2003) argued that standardised CPUE might be able to relate to the changes of abundance in a fully exploited fishery such as PAU 7 and PAU 5D.

Analysis of CPUE currently relies on paua Catch Effort Landing Return (PCELR) forms, which record daily fishing time and catch per diver on a relatively large spatial scale. These data are likely to remain the basis for stock assessments and formal management in the medium term. Since October 2010, a dive-logger data collection programme has been initiated to achieve fine-scale monitoring of paua fisheries (Neubauer & Abraham 2014, Neubauer et al. 2015). The use of the data loggers by paua divers and ACE holders has been steadily increasing over the last three years. Using fishing data logged at fine spatial and temporal scales could substantially improve effort calculations and the resulting CPUE indices and allow complex metrics such as spatial CPUE to be developed (Neubauer 2015). Data from the loggers have been analysed to provide comprehensive descriptions of the spatial extent of the fisheries and insight on relationships between diver behaviour, CPUE, and changes in abundance on various spatial and temporal scales (Neubauer & Abraham 2014, Neubauer et al. 2015). However the data-loggers can potentially change how the divers operate such that they may become more effective in their fishing operations (the divers become capable of avoiding areas that have been heavily fished or that have relatively low CPUE without them having to go there to discover this), therefore changing the meaning of diver CPUE (Butterworth et al. 2015).

The current basis for the assumption of natural mortality is somewhat *ad hoc*, and the prior used is considered to be unduly informative (Butterworth et al. 2015). Although sensitivity runs were done with different *a priori* assumptions of M, it was clear that the estimates were highly influenced by this assumption. This suggests that a better understanding of this parameter/dynamic would be likely to reduce a large component of uncertainty in this assessment.

Heterogeneity in growth can be a problem for length based models (Punt 2003). Variation in growth is addressed to some extent by having a stochastic growth transition matrix based on increments observed in multiple areas; similarly the length frequency data are integrated across samples from many places. Relative weights were investigated, so that more productive areas were better represented in the model. However, this yielded growth which was thought by the SFWG to be unreasonable.

The model treats the whole of the assessed area of PAU 5D as if it were a single stock with homogeneous biology, habitat and fishing pressures. The model assumes homogeneity in recruitment and natural mortality, and that growth has the same mean and variance. However, it is known that localised variation and processes are important for paua (Breen et al. 1982). For instance, if some local stocks are fished very hard and others are not fished, recruitment failure can result because of the depletion of spawners. Spawners must breed close to each other and the dispersal of larvae is unknown and may be limited. Recruitment failure is a common observation in overseas abalone fisheries, suggesting that local processes may decrease recruitment, an effect that the current model cannot account for. The biology of paua mentioned above adds a great deal of uncertainty into the model and future improvements could include a more spatially explicit model or simulations to understand the effects of ignoring such spatially variable processes.

The SFWG also discussed the possibility of a future issue regarding bias in the CSLF catch sampling data. This comes about from the sampling protocol of measuring the shells once paua have been harvested. Recently there has been a suggestion that the live export market is increasing which favours large fish. Under the current sampling protocol these large fish may be missing in the length frequency distributions which will bias the CSLFs. This should be discussed and or investigated in the next assessment for this stock.

5. ACKNOWLEDGMENTS

This work was supported by a contract from the Ministry for Primary Industries (PAU201601 Objective 1). Thank you to Paul Breen for developing the stock assessment model that was used in this assessment and for the use of major proportions of the 2006 report for this update. Thank you to the

Shellfish Working Group for all the advice provided throughout the assessment process. Thank you to Reyn Naylor and Matt Dunn for reviewing the draft report.

6. REFERENCES

Abraham, E.R.; Neubauer, P. (2015). Relationship between small-scale catch-per-unit-effort and abundance in New Zealand abalone (pāua, *Haliotis iris*) fisheries. PeerJPrePrints, 3, e1733. Doi:10.7287/peerj/preprints.1388v2.

Andrew, N.L.; Breen, P.A.; Naylor, J.R.; Kendrick, T.H.; Gerring, P. (2000). Stock assessment of paua (*Haliotis iris*) in PAU 7 in 1998–99. *New Zealand Fisheries Assessment Report 2000/49*. 40 p.

Breen, P.A.; Adkins, B.; Station, P.B. (1982). Observations of abalone populations on the north coast of British Columbia, July 1980. Department of Fisheries and Oceans, Resource Services Branch, Pacific Biological Station.

Breen, P.A.; Andrew, N.L.; Kendrick, T.H. (2000a). Stock assessment of paua (*Haliotis iris*) in PAU 5B and PAU 5D using a new length-based model. *New Zealand Fisheries Assessment Report 2000/33*. 37 p.

Breen, P.A.; Andrew, N.L.; Kendrick, T.H. (2000b). The 2000 stock assessment of paua (*Haliotis iris*) in PAU 5B using an improved Bayesian length-based model. *New Zealand Fisheries Assessment Report 2000/48*. 36 p.

Breen, P.A.; Andrew, N.L.; Kim, S.W. (2001). The 2001 stock assessment of paua (*Haliotis iris*) in PAU 7. *New Zealand Fisheries Assessment Report 2001/55*. 53 p.

Breen, P.A.; Kim, S.W. (2003). The 2003 stock assessment of paua (*Haliotis iris*) in PAU 7. *New Zealand Fisheries Assessment Report 2003/35.* 112 p.

Breen, P.A.; Kim, S.W. (2004a). The 2004 stock assessment of paua (*Haliotis iris*) in PAU 4. *New Zealand Fisheries Assessment Report 2004/55.* 79 p.

Breen, P.A.; Kim, S.W. (2004b). The 2004 stock assessment of paua (*Haliotis iris*) in PAU 5A. *New Zealand Fisheries Assessment Report 2004/40*. 86 p.

Breen, P.A.; Kim, S.W. (2005). The 2005 stock assessment of paua (*Haliotis iris*) in PAU 7. *New Zealand Fisheries Assessment Report 2005/47.* 114 p.

Breen, P.A.; Kim, S.W. (2007). The 2006 stock assessment of paua (*Haliotis iris*) stocks PAU 5A (Fiordland) and PAU 5D (Otago). *New Zealand Fisheries Assessment Report 2007/09*. 164 p.

Breen, P.A.; Kim, S.W.; Andrew, N.L. (2003). A length-based Bayesian stock assessment model for abalone. *Marine and Freshwater Research 54(5):* 619–634.

Breen, P.A.; Smith, A.N.H. (2008a). The 2007 assessment for paua *(Haliotis iris)* stock PAU 5B (Stewart Island). *New Zealand Fisheries Assessment Report 2008/05.*

Breen, P.A.; Smith, A.N.H. (2008b). Data used in the 2007 assessment for paua (*Haliotis iris*) stock PAU 5B (Stewart Island). *New Zealand Fishery Assessment Report 2008/6*. 45 p.

Butterworth, D.; Haddon, M.; Haist, V.; Helidoniotis, F. (2015). Report on the New Zealand Paua stock assessment model; 2015. *New Zealand Fisheries Science Review 2015/4*. 31 p

Cordue, P.L. (2009). Analysis of PAU5A dive survey data and PCELR catch and effort data. Final report for SeaFIC and PauaMAC5. (Unpublished report held by SeaFIC.)

Dunn, A.; Harley, S.; Doonan, I.J; Bull, B. (2000). Calculation and interpretation of catch-per-unit-effort (CPUE) indices. *New Zealand Fisheries Assessment Report. 2000/1*. 44 p.

Francis, R.I.C.C. (2011). Data weighting in statistical fisheries stock assessment models. *Canadian Journal of Fisheries and Aquatic Sciences* 68: 1124–1138.

Fu, D. (2012). The 2011 stock assessment of paua (*Haliotis iris*) for PAU 7. *New Zealand Fisheries Assessment Report 2012/27*. 56 p.

Fu, D. (2013). The 2012 stock assessment of paua (*Haliotis iris*) for PAU 5D. *New Zealand Fisheries Assessment Report 2013/57*. 56 p.

Fu, D. (2014a). The 2013 stock assessment of paua (*Haliotis iris*) for PAU 5B. *New Zealand Fisheries Assessment Report* 2014/ 45.

Fu, D. (2014b). The 2013 stock assessment of paua (*Haliotis iris*) for PAU 3. *New Zealand Fisheries Assessment Report* 2014/45. 51 p.
Fu, D. (2015a). The 2014 stock assessment of paua (Haliotis iris) for Chalky and South Coast in PAU 5A. *New Zealand Fisheries Assessment Report* 2015/64. 63 p.
Fu, D. (2015b). The 2014 stock assessment of paua (*Haliotis iris*) for Milford, George, Central, and Dusky in PAU 5A. *New Zealand Fisheries Assessment Report* 2015/65. 63 p.
Fu, D. (2016). The 2015 stock assessment of paua (*Haliotis iris*) for PAU 7. *New Zealand Fisheries Assessment Report*, 2016/35. 52 p.
Fu, D.; McKenzie, A. (2010a). The 2010 stock assessment of paua (*Haliotis iris*) for Chalky and South Coast in PAU 5A. *New Zealand Fisheries Assessment Report 2010/36.* 63 p.
Fu, D.; McKenzie, A. (2010b). The 2010 stock assessment of paua (*Haliotis iris*) for Milford, George, Central, and Dusky in PAU 5A. *New Zealand Fisheries Assessment Report 2010/46*. 55 p.
Fu, D.; McKenzie. A; Naylor, R. (2010). Summary of input data for the 2010 PAU 5A stock assessment. *New Zealand Fisheries Assessment Report 2010/35*. 58 p.
Fu, D.; McKenzie, A.; Naylor, J.R. (2012). Summary of input data for the 2011 PAU 7 stock assessment. *New Zealand Fisheries Assessment Report* 2012/26. 46 p.
Fu, D.; McKenzie, A; Naylor, R. (2013). Summary of input data for the 2012 PAU 5D stock assessment. *New Zealand Fisheries Assessment Report* 2013/56. 47 p.
Fu, D.; McKenzie, A; Naylor, R. (2014a). Summary of input data for the 2013 PAU 5B stock assessment. *New Zealand Fisheries Assessment Report* 2014/43. 61 p.
Fu, D.; McKenzie, A; Naylor, R. (2014b). Summary of input data for the 2013 PAU 3 stock assessment. *New Zealand Fisheries Assessment Report* 2014/42. 45 p.
Fu, D.; McKenzie, A; Naylor, R. (2015). Summary of input data for the 2014 PAU 5A stock assessment. *New Zealand Fisheries Assessment Report 2015/68*. 88 p
Fu, D.; McKenzie, A; Naylor, R. (2016). Summary of input data for the 2015 PAU 7 stock assessment. *New Zealand Fisheries Assessment Report* 2016/38. 86 p.
Fu, D.; McKenzie, A; Marsh, C. (2017). Summary of input data for the 2016 PAU 5D stock assessment. *New Zealand Fisheries Assessment Report 2017/32* 79 p.
Haist, V. (2010). Paua research diver survey: review of data collected and simulation study of survey method. *New Zealand Fisheries Assessment Report 2010/38*. 54 p.
Kim, S.W.; Bentley, N.; Starr, P.J.; Breen, P.A. (2004). Assessment of red rock lobsters (*Jasus edwardsii*) in CRA 4 and CRA 5 in 2003. *New Zealand Fisheries Assessment Report 2004/8.* 165 p.
McKenzie, A.; Smith, A.N.H. (2009a). The 2008 stock assessment of paua (*Haliotis iris*) in PAU 7. *New Zealand Fisheries Assessment Report 2009/34.* 84 p.
McKenzie, A.; Smith, A.N.H. (2009b). Data inputs for the PAU 7 stock assessment in 2008. *New Zealand Fisheries Assessment Report 2009/33.* 34 p.
McShane, P.E.; Mercer, S.F.; Naylor, J.R. (1994). Spatial variation and commercial fishing of the New Zealand paua (*Haliotis iris* and *H. australis*). *New Zealand Journal of Marine and Freshwater Research* 28: 345–355.
McShane, P.E.; Mercer, S.; Naylor, J.R.; Notman, P.R. (1996). Paua (*Haliotis iris*) fishery assessment in PAU 5, 6, and 7. New Zealand Fisheries Assessment Research Document 96/11. 35 p. (Unpublished report held in NIWA library, Wellington.)
Neubauer, P. (2015). Alternative CPUE indices for PAU7, 11 p. Unpublished report prepared for the Shellfish Working Group.
Neubauer, P.; Abraham, E. (2014). Using GPS logger data to monitor change in the PAU 7 pāua (*Haliotis iris*) fishery. *New Zealand Fisheries Assessment Report 2014/31*. 18 p.
Neubauer, P.; Abraham, E.; Know, C.; Richard, Yvan. R. (2015). Assessing the performance of paua (*Haliotis iris*) fisheries using GPS logger data. *New Zealand Fisheries Assessment Report 2015/71.*
Punt, A.E. (2003). The performance of a size-structured stock assessment method in the face of spatial heterogeneity in growth. *Fisheries Research 65:* 391–409.
Schiel, D.R. (1989). Paua fishery assessment 1989. New Zealand Fisheries Assessment Research Document 89/9: 20 p. (Unpublished report held in NIWA library, Wellington, New Zealand.)

Schiel, D.R. (1992). The paua (abalone) fishery of New Zealand. *In:* Abalone of the world: Biology, fisheries and culture. Shepherd, S.A.; Tegner, M.J.; Guzman del Proo, S. (eds.) pp. 427–437. Blackwell Scientific, Oxford.

Schiel, D.R.; Breen, P.A. (1991). Population structure, ageing and fishing mortality of the New Zealand abalone *Haliotis iris*. *Fishery Bulletin 89*: 681–691.

Schnute, J. (1985). A General Theory for Analysis of Catch and Effort Data. *Canadian Journal of Fisheries and Aquatic Sciences 42(3)*: 414–429.

Shepherd, S.A.; Rodda, K.R.; Vargas, K.M. (2001). A chronicle of collapse in two abalone stocks with proposals for precautionary management. *Journal of Shellfish Research 20:* 843–856.

Table 1: Actual sample sizes, initial sample sizes determined for the multinomial likelihood, and model weighted sample sizes for the PAU 5D commercial catch sampling length frequencies from the base model (0.0). A descriptions of the model runs is summarised in Table 4.

Fishing year	Actual sample size	Initial sample size	0.0
1998	2 206	420	14
2002	5 242	662	23
2003	5 907	790	27
2004	3 277	490	17
2007	2 060	446	15
2009	3 270	798	28
2010	3 618	1157	40
2011	1 707	647	22
2012	2 549	673	23
2013	4 121	672	23
2014	5 254	1078	37
2015	3 898	877	30

Table 2: Base case model specifications: for estimated parameters, the phase of estimation, type of prior, (U, uniform; N, normal; LN, lognormal), mean and CV of the prior, lower bound and upper bound.

Parameter	Phase	Prior	μ	CV	Lower	Upper
ln($R0$)	1	U	–	–	5	50
M	3	LN	0.1	0.1	0.01	0.5
g_1	2	U	–	–	0.01	150
g_2	2	U	–	–	0.01	150
g_{50}	2	U			0.01	150
$g_{50\text{-}95\%}$	2	U	–	–	0.01	150
g_{max}	1	U	–	–	0.01	50
α	2	U			0.01	10
β	2	U	–	–	0.01	10
$Ln(q^I)$	1	U	–	–	-30	0
$Ln(q^J)$	1	U	–	–	-30	0
L_{50}	1	U	–	–	70	145
$L_{95\text{-}50}$	1	U	–	–	1	50
D_{50}	2	U	–	–	70	145
$D_{95\text{-}50}$	2	U	–	–	0.01	50
D_s	1	U	–	–	0.01	10
ε	1	N	0	0.4	-2.3	2.3

Table 3: Values for fixed quantities for base case model.

Variable	Value
L_1	75
L_2	120
a	2.99E-08
b	3.303
U^{max}	0.80
σ_{min}	1
σ_{obs}	0.25
$\widetilde{\sigma}$	0.2
H	0.75

Table 4: **Summary descriptions of base case (0.0) and sensitivity model runs.**

Model	Description
0.0	Exponential model, tag-recapture unweighted, M prior lognormal (mean = 0.1,CV = 0.1), tag data > 70mm
0.0b	Model 0.0, M prior lognormal (mean = 0.15, CV = 0.1)
0.0e	Model 0.0, doubled the CV for the CPUE
0.0h	Model 0.0, fix CPUE shape parameter (h = 0.5)
0.1	inverse-logistic model, tag-recapture unweighted, M prior lognormal (mean = 0.1, CV = 0.1), all tag data

Table 5: MPD estimates for base case and sensitivity trials. "–" indicates that parameter is fixed and likelihood contributions were not used when datasets were removed. SDNRs for CSLF were calculated from mean length. "Weights" means CV for CPUE indices and mean sample size for length frequency data.

Model runs	0.0	0.0b	0.0e	0.0h	0.1
Parameters					
ln(R0)	13.8	14.0	13.7	13.6	13.8
M	0.14	0.18	0.13	0.12	0.13
L_{50}	84.2	84.2	84.2	84.2	84.2
L_{95-50}	19.1	19.1	19.1	19.1	19.1
D_{50}	125.1	125.30	124.6	126.5	123.7
D_{95-50}	5.8	6.14	5.9	6.8	4.8
D_{shift}	0.4	0.47	0.6	0.3	0.4
T_{50}	–	–	–	–	–
T_{95-50}	–	–	–	–	–
$\ln(q^{I})$	-13.0	-12.9	-13.2	-4.1	-13.4
$\ln(q^{I2})$	-12.7	-12.7	-12.7	-3.9	-13.2

Table 5. cont.

$\ln(q^J)$	–	–	–	–	–
h	–	–	–	0.5	–
g_α	28.3	27.9	28.19	27.6	–
g_β	7.0	7.1	6.97	7.1	–
g_{max}	–	–	–	–	20.2
$g_{50\%}$	–	–	–	–	113.0
$g_{50\text{-}95\%}$	–	–	–	–	38.6
a	1.24	1.20	1.23	1.2	1.54
b	0.55	0.57	0.56	0.6	0.43
Indicators					
B0	2367	2109	2542	2614	2529
Bcurrent	771	848	743	566	956
Bcurrent/B0	0.33	0.40	0.29	0.22	0.38
rB0	1988	1676	2185	2288	2144
rBcurrent	459	476	455	321	629
rBcurrent/rB0	0.23	0.28	0.21	0.14	0.29
Ucurrent	0.22	0.23	0.23	0.33	0.15
Likelihoods					
CPUE	-11.1	-13.1	-3.7	-10.349	-11.7
PCPUE	-19.6	-19.6	-11.6	-17.8	-20.0
RDSI	–	–	–	–	–
CSLF	9.2	8.6	8.2	6.927	8.7
RDLF	–	–	–	–	–
Tags	659.9	659.7	659.9	659.7	767.7
Maturity	-53.0	-53.0	-53.0	-53.0	-53.0
Prior on M	4.9	0.1	1.5	-0.1	1.4
Prior on ε	8.2	5.6	4.1	4.9	6.1
U penalty	0.0	0.0	0.0	0	0.0
ε penalty	0.0	0.0	0.0	0.0	0.0
Total	598.6	588.4	605.5	590.3	699.1
Weights					
CPUE	0.10	0.10	0.20	0.10	0.10
PCPUE	0.08	0.08	0.16	0.08	0.08
RDSI	–	–	–	–	–
CSLF	25	26	23	15	16
RDLF	–	–	–	–	–
SDNRs					
CPUE	0.96	0.77	0.88	1.02	0.90
PCPUE	0.77	0.78	0.52	0.92	0.74
RDSI	–	–	–	–	–
CSLF	1.00	1.00	1.00	1.02	1.00
RDLF	–	–	–	–	–
Tags	1.01	1.01	1.00	1.00	1.00
Maturity	1.08	1.08	1.08	1.09	1.08
Maturity	0.66	0.66	0.66	0.66	0.66

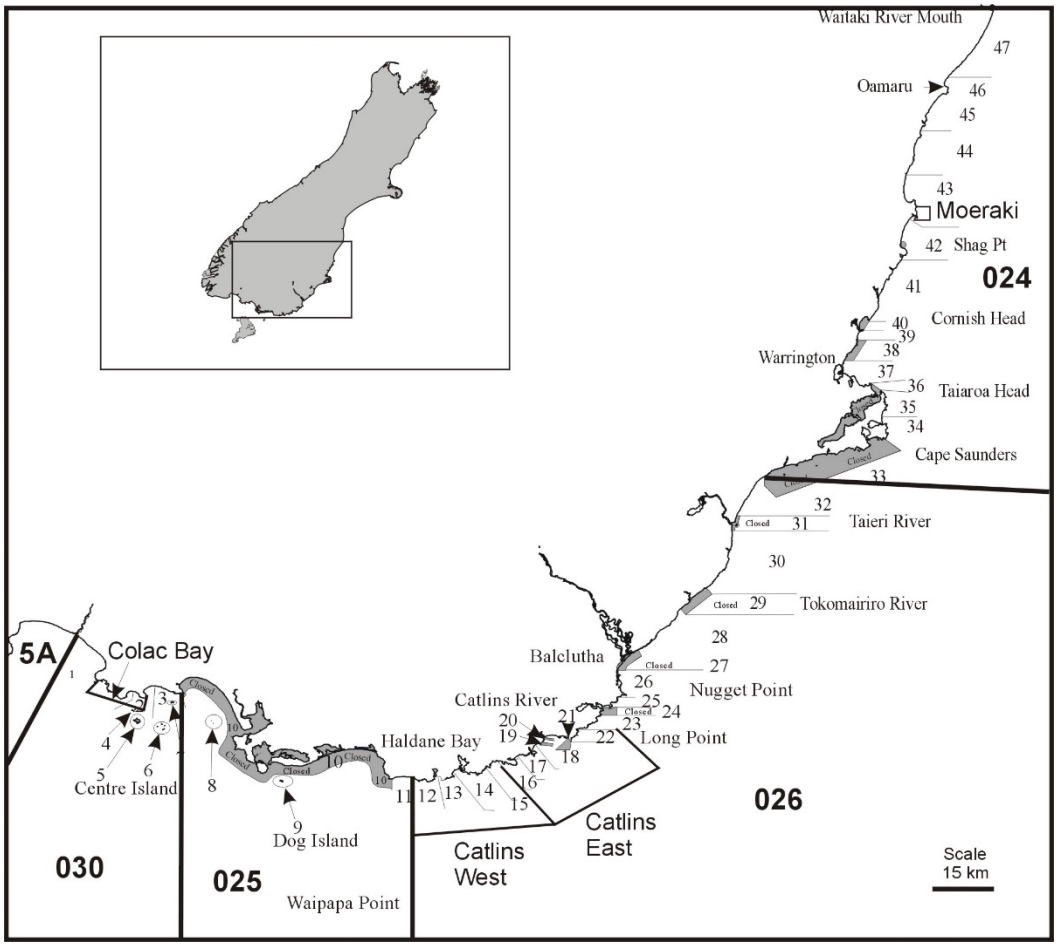

Figure 1: Map of PAU 5D showing the boundaries of the General Statistical Areas and the new finer scale Paua Statistical Areas.

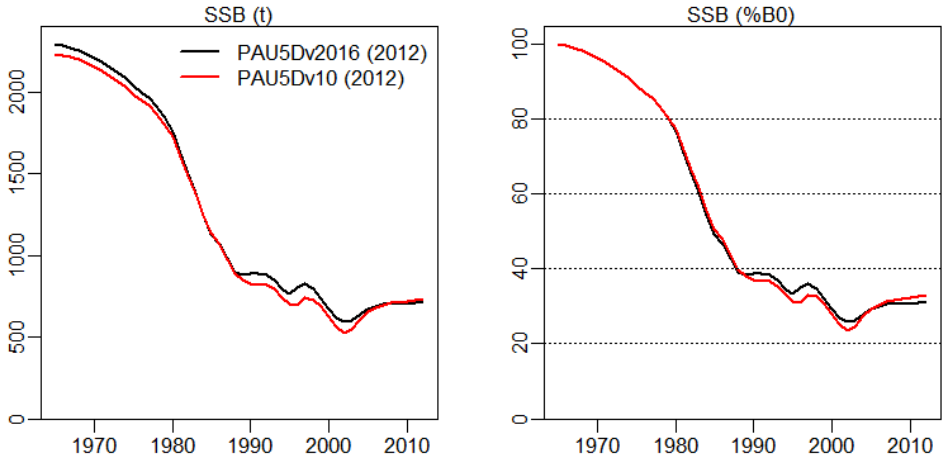

Figure 2: Comparison between the previous base model for this stock (PAU5Dv10 (2012)) and the updated model (PAU5Dv2016 (2012)).

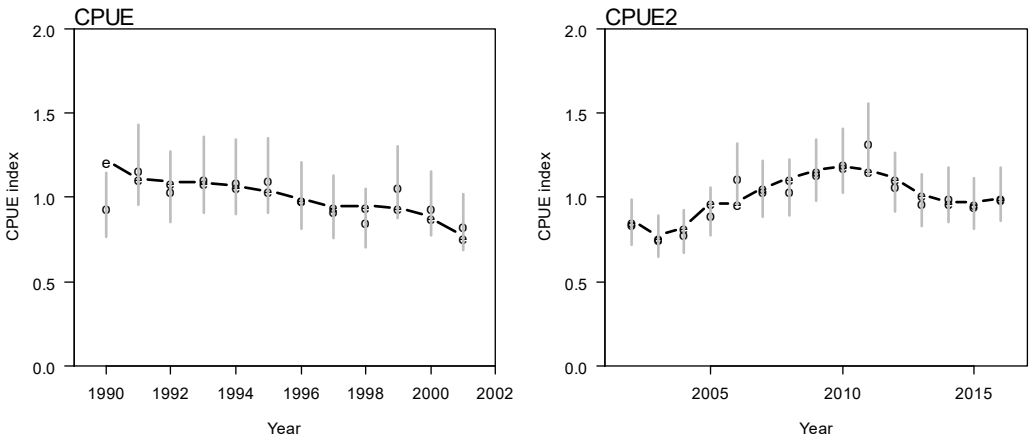

Figure 3: Fits to the CPUE indices 1990–2001 (left) and 2002–2016 indices (right), for MPD 0.0.

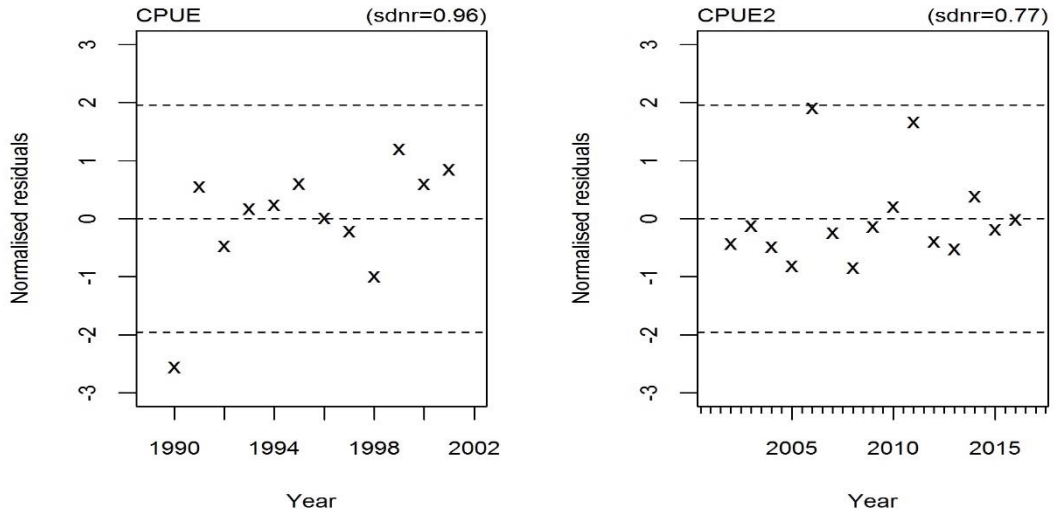

Figure 4: Normalised residuals from fits to the two CPUE datasets for MPD 0.0.

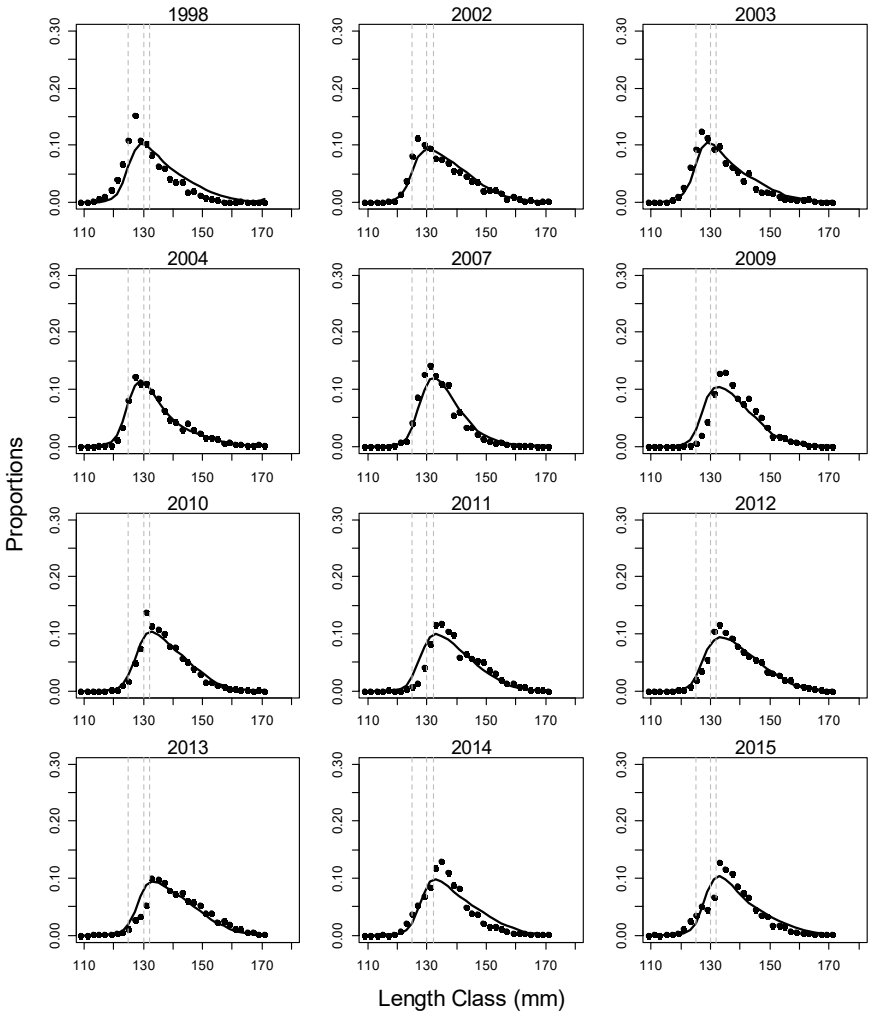

Figure 5: Fits to the CSLF data 1998, 2002, 2002–2004, 2007, 2009–2015 for MPD 0.0.

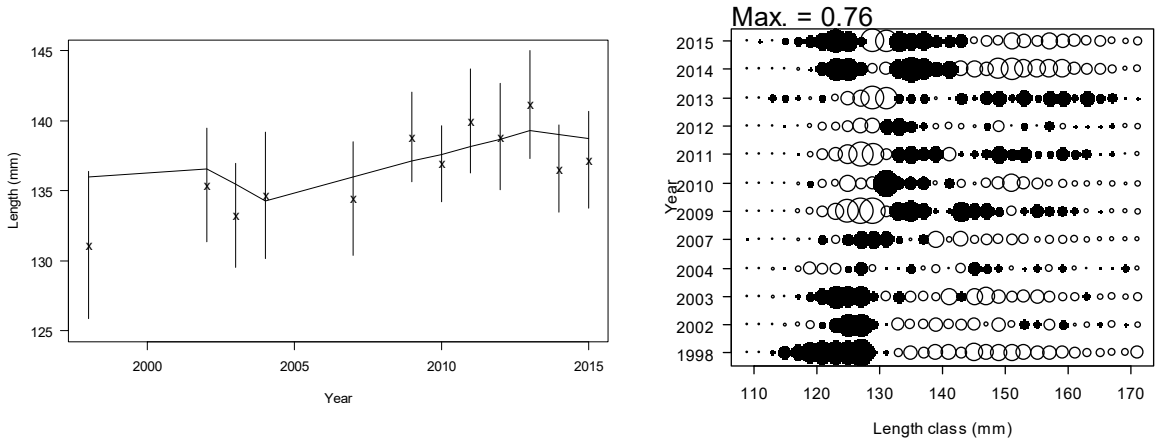

Figure 6: Observed and predicted mean length by year for the CSLF (left) and normalised residuals from fits MPD 0.0. The size of the circle is proportional to the value. Black circles represent negative residuals and white circles represent positive residuals.

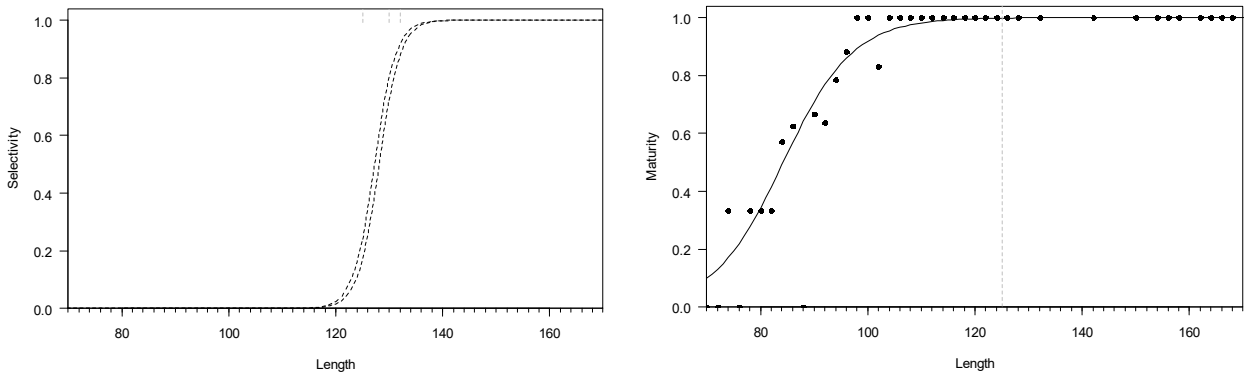

Figure 7: Estimated commercial fishing selectivity (left) and fits to the length-at-maturity data (right) for MPD 0.0. Vertical lines represents minimum harvest sizes of 125, 130, and 132 mm (left).

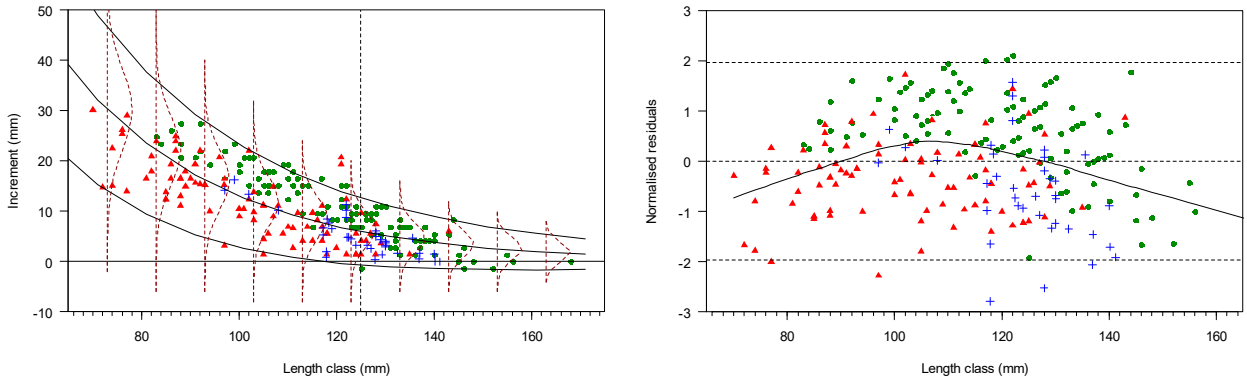

Figure 8: Estimated exponential growth curve for MPD 0.0 (left) and normalised residuals from the fit (right). For the fits to the tag-recapture data (left), dots are observed mean annual increments; the lines are the fitted growth curves with 95% confidence intervals at selected sizes. The line on the right is smoother to show the general trend. Green dots, Catlins west; red triangles, Catlins east; blue crosses, east coast.

Figure 9: CPUE fits between the base case model (0.0) and the sensitivity run with doubled CV on CPUE (0.0e).

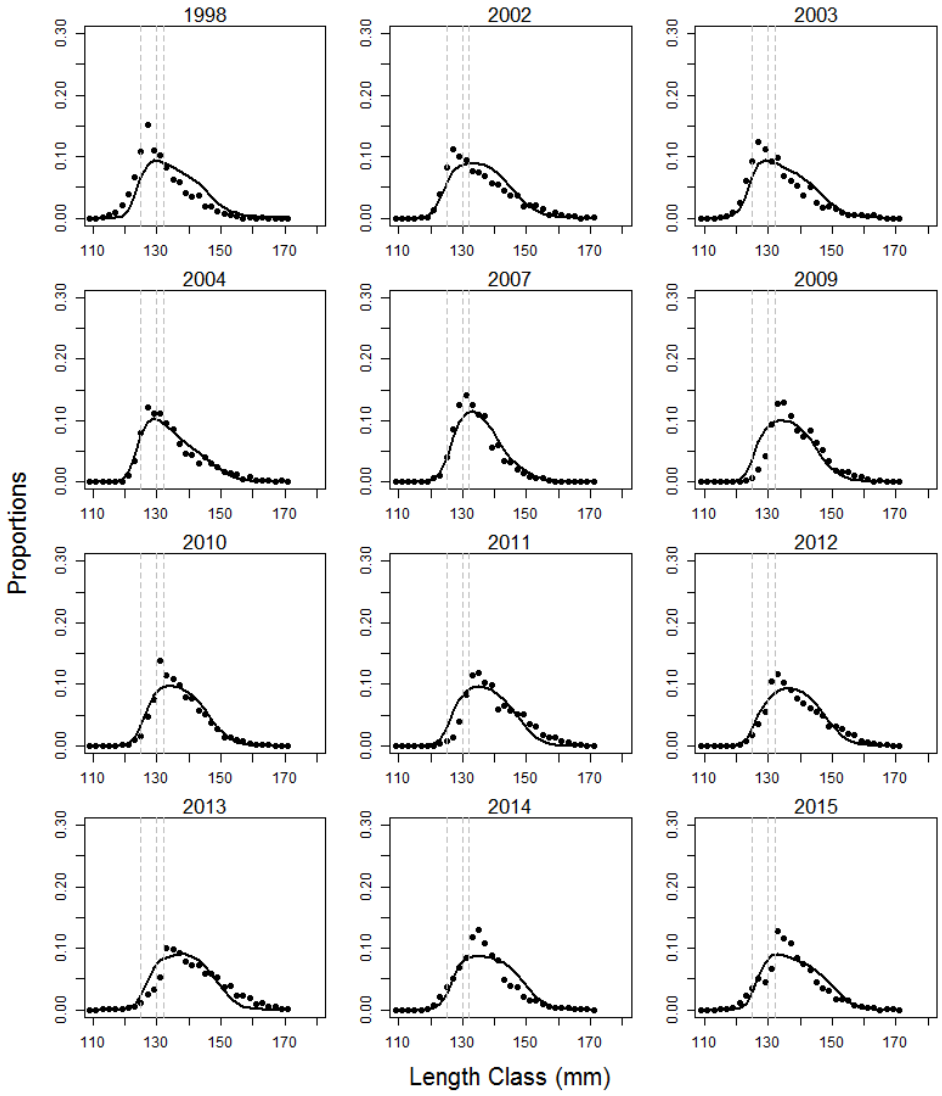

Figure 10: Fits to the CSLF data 1998, 2002, 2002–2004, 2007, 2009–2015 for MPD 0.1 (inverse logistic growth model).

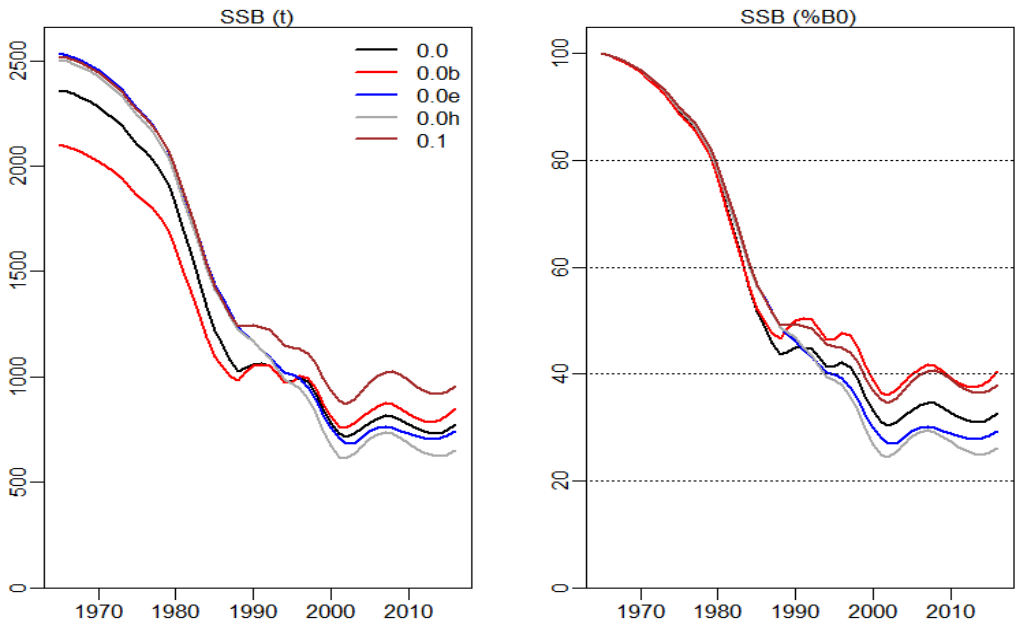

Figure 11: Left panel is the spawning stock biomass (SSB) through time for the base case and sensitivity runs presented in this assessment. The right-hand panel is SSB expressed as % B_0.

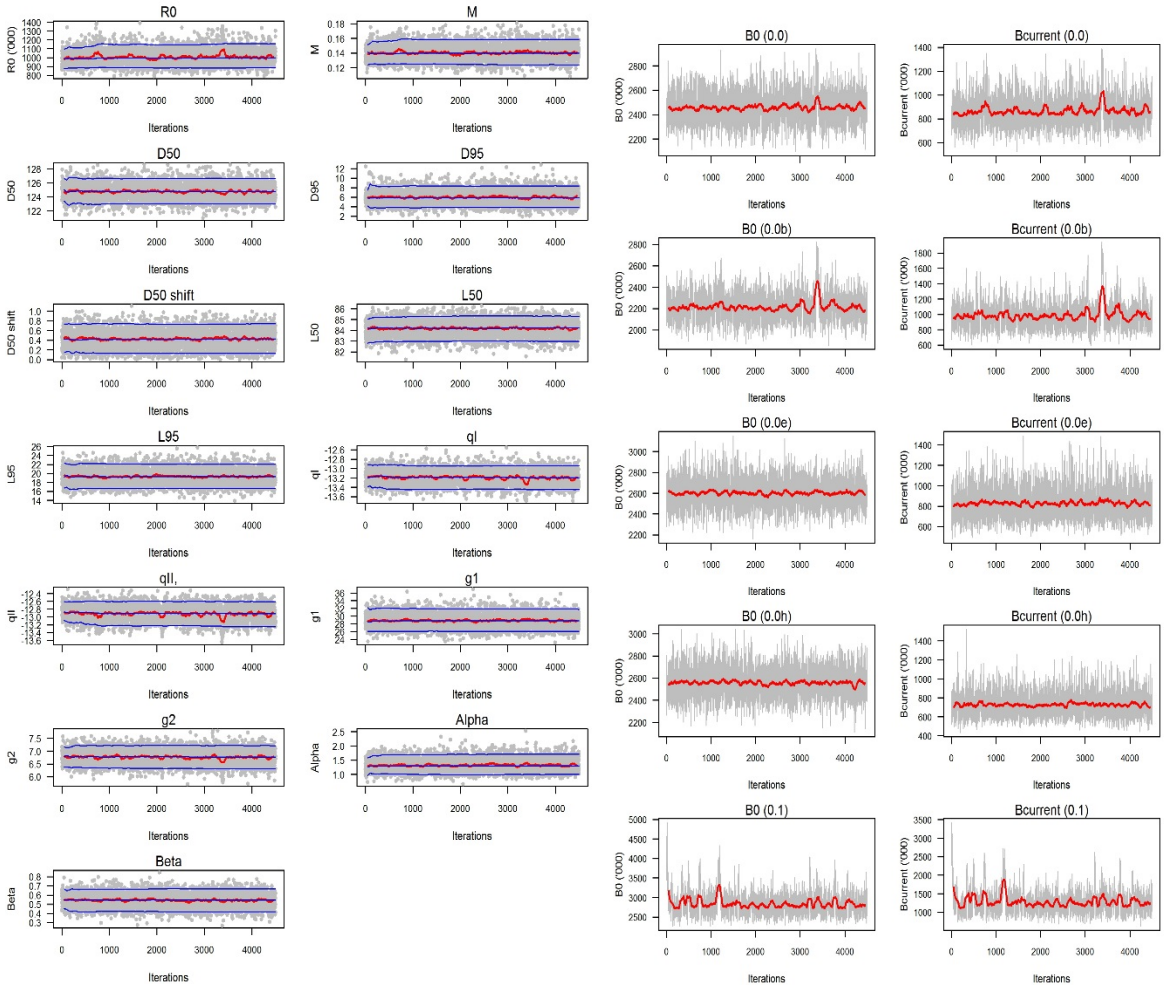

Figure 12: Traces of posterior samples for estimated parameters for MCMC 0.0 (base case) (left), and for biomass indicators for MCMC 0.0, 0.0b, 0.0e, 0.0h and 0.1 (right). Blue lines are running 5, 50, and 95% quantiles of the chain and red lines are the moving average of the chain.

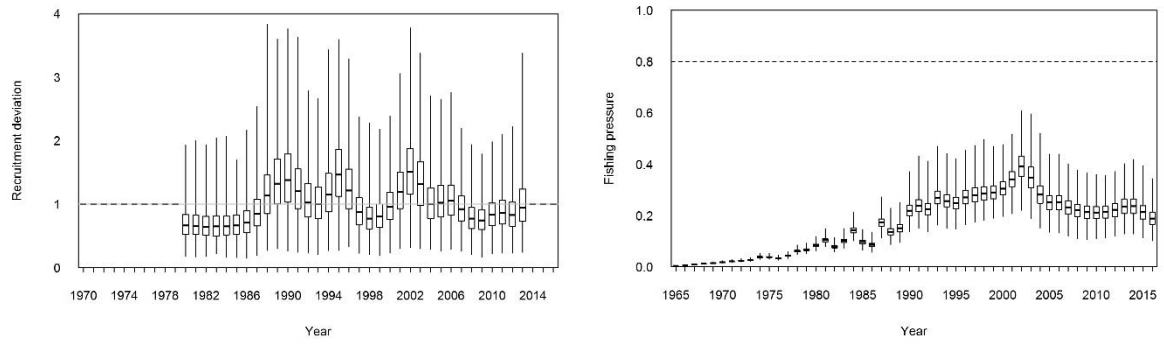

Figure 13: Posterior distributions of recruitment deviations (left), and exploitation rates (right) for MCMC 0.0. The box shows the median of the posterior distribution (horizontal bar), the 25th and 75th percentiles (box), with the whiskers representing the full range of the distribution. Recruitment deviations were estimated for 1980–2012, and fixed at 1 for other years. Maximum exploitation rate was assumed to be 0.8.

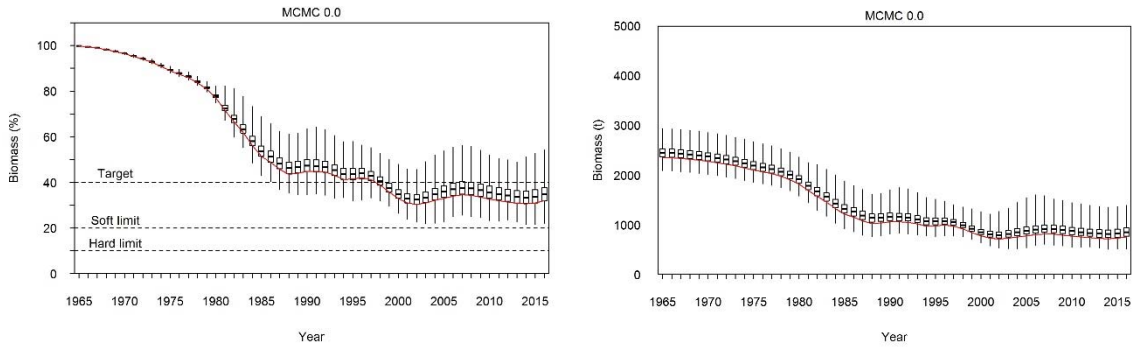

Figure 14: Posterior distributions of spawning stock biomass and spawning stock biomass as a percentage of virgin level from MCMC 0.0. The box shows the median of the posterior distribution (horizontal bar), the 25th and 75th percentiles (box), with the whiskers representing the full range of the distribution. The red line shows the MPD equivalent for reference.

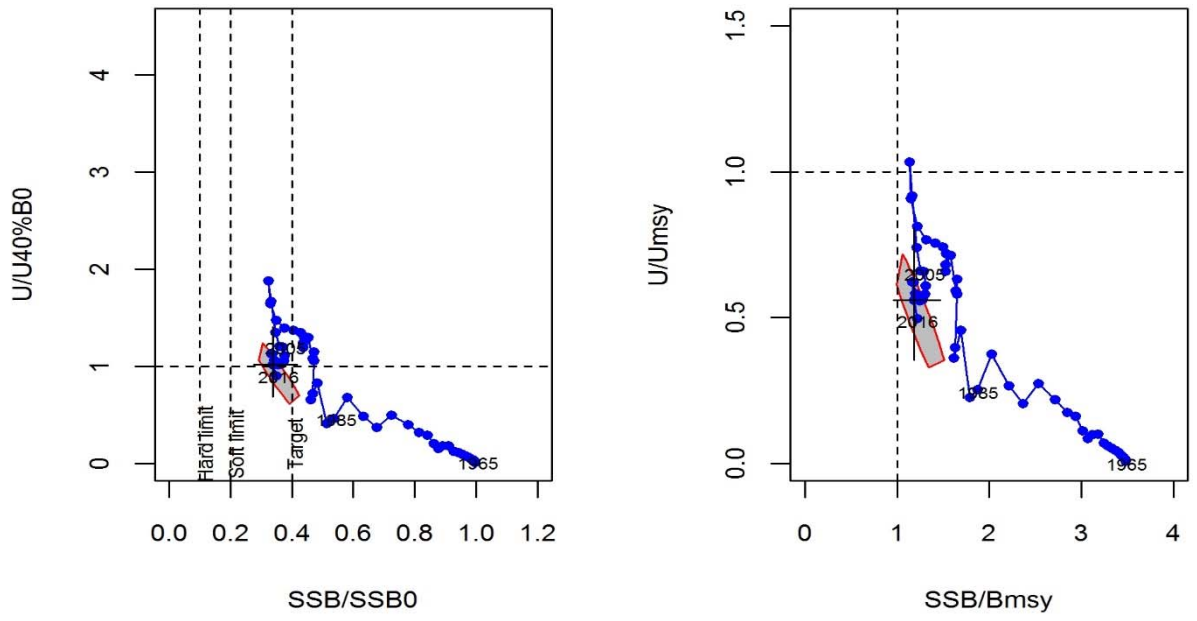

Figure 15: Trajectory of exploitation rate as a ratio of $U_{\%40B0}$ and spawning stock biomass as a ratio of B_0 (left), and exploitation rate as a ratio of U_{msy} and spawning stock biomass as a ratio of B_{msy} from the start of assessment period (right) 1965 to 2016 for MCMC 0.0 (base case). The vertical lines at 10%, 20% and 40% B_0 represent the soft limit, the hard limit, and the target. Estimates are based on MCMC median and the 2016 90% marginal CI is shown by the cross line, and joint CI is shown by the grey area.

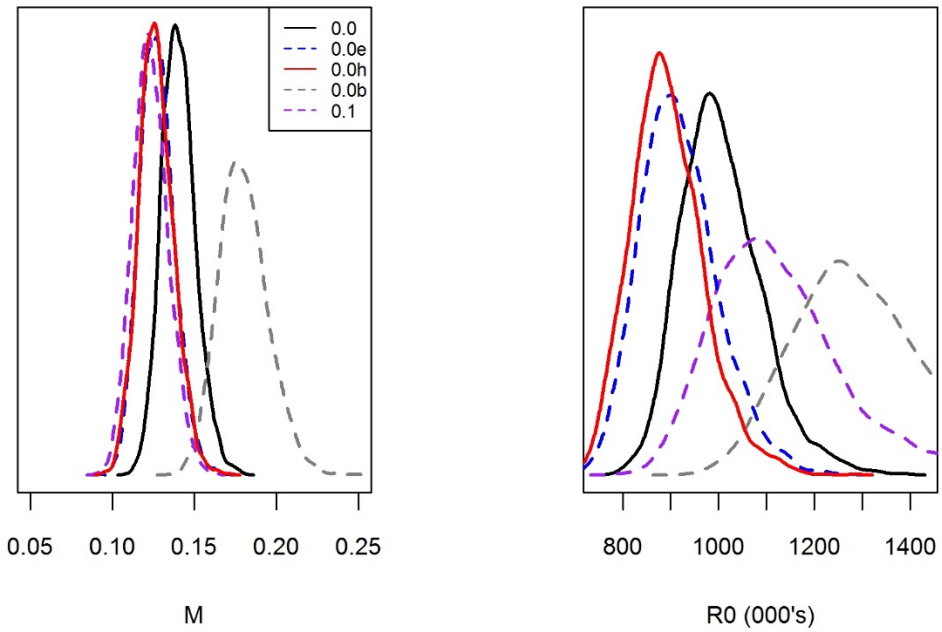

Figure 16: Comparison of marginal posterior distribution of the natural mortality parameter (left). The right panel shows the comparison of the marginal posterior for R0 across base case and sensitivity models.

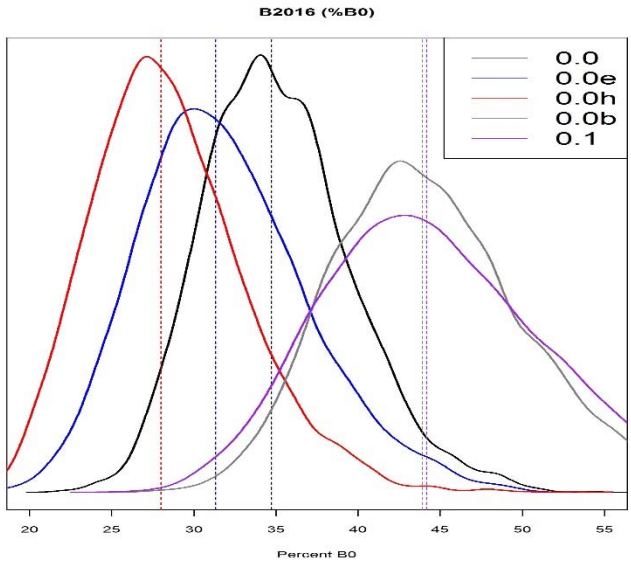

Figure 17: Comparison of marginal posterior of $\%B_{current}$ between MCMC 0.0, 0.0b, 0.0e 0.0h, and 0.1. Dashed vertical line indicates the median value.

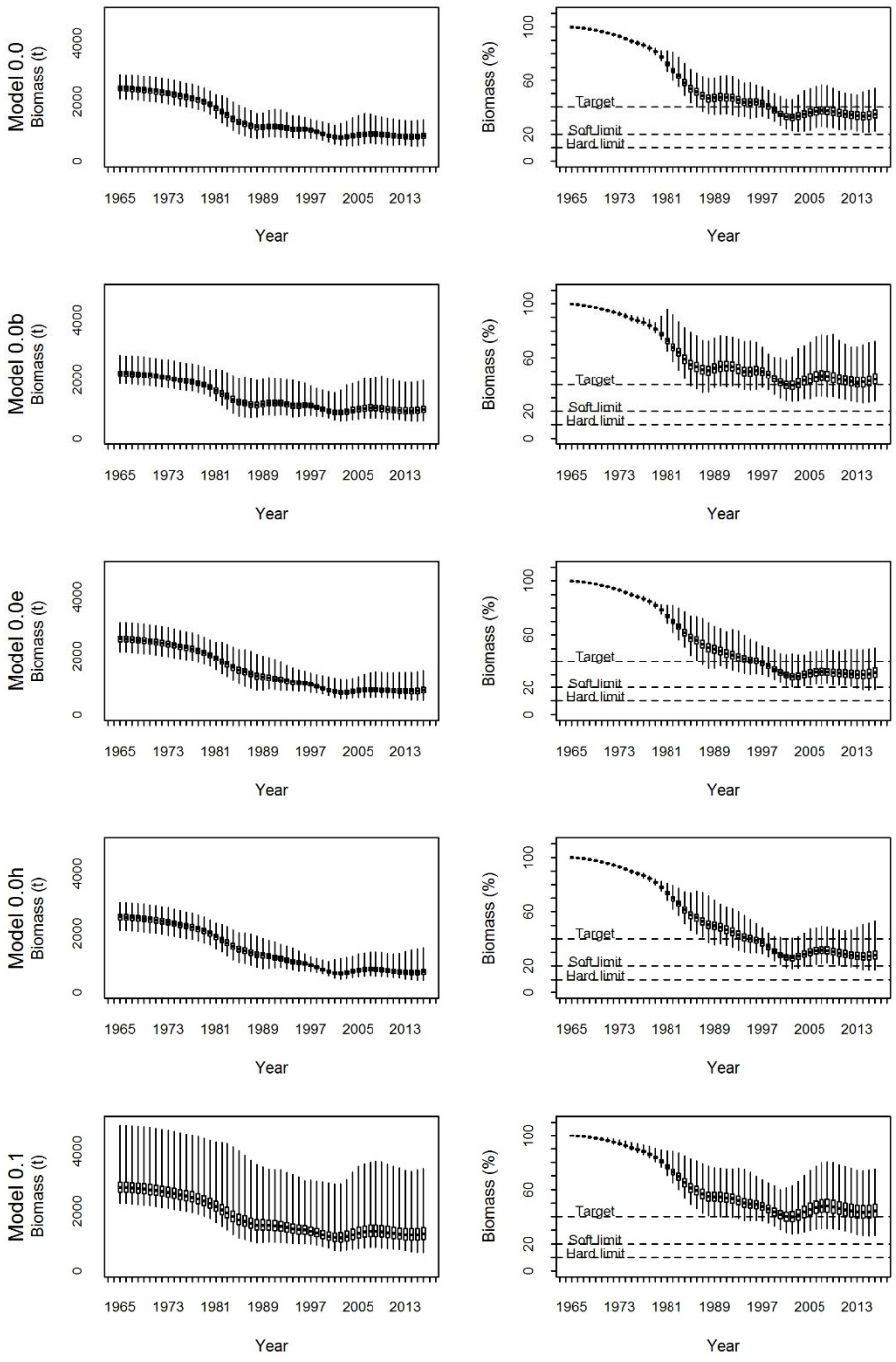

Figure 18: Posterior distributions of spawning stock biomass as a percentage of virgin level from MCMC 0.0, 0.0b, 0.0e, 0.0h, and 0.1. The box shows the median of the posterior distribution (horizontal bar), the 25th and 75th percentiles (box), with the whiskers representing the full range of the distribution.

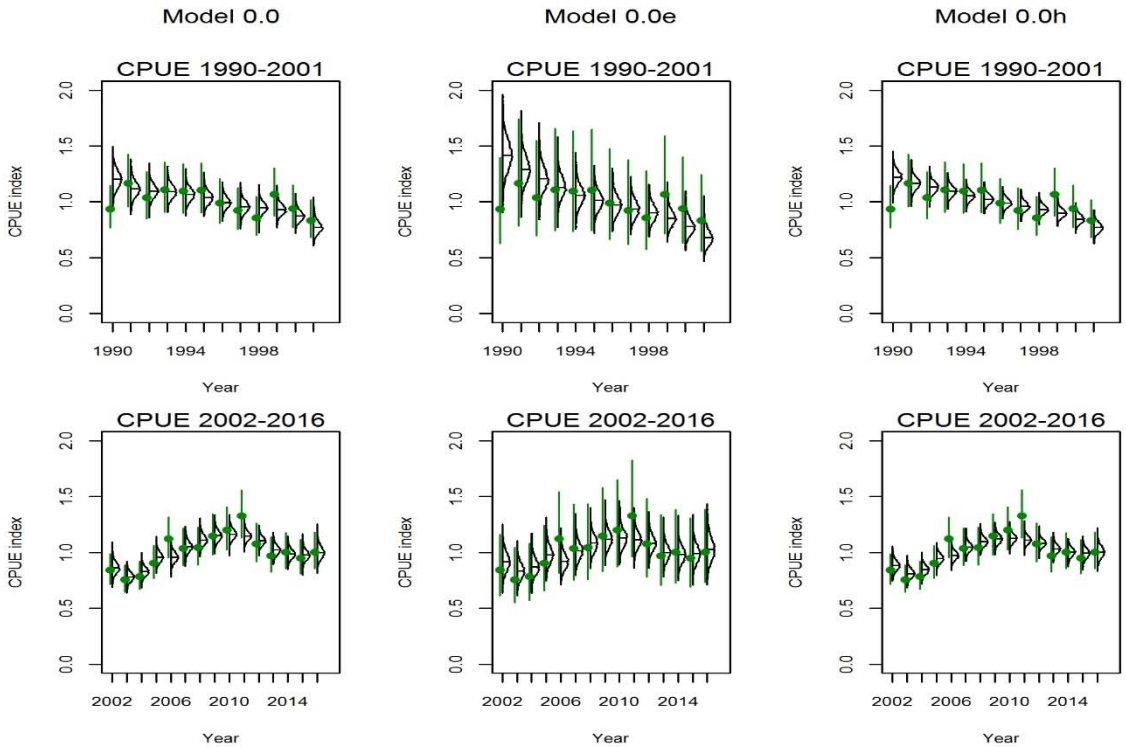

Figure 19: Posterior distributions of model predicted CPUE indices for 1990–2016 for MCMC 0.0, 0.0e and 0.0h (Medians are shown as horizontal lines). Dots are observed CPUE indices and vertical lines are 95% confidence intervals.

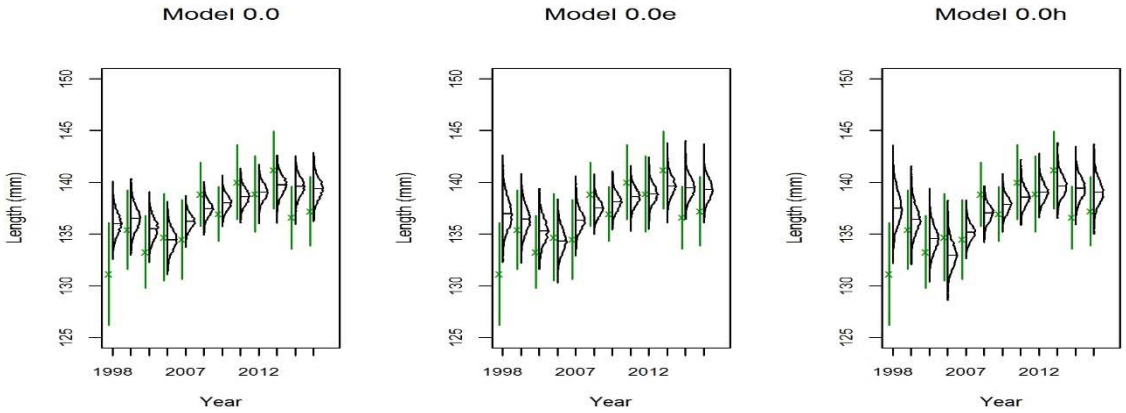

Figure 20: Posterior distributions of model predicted mean CSLF indices for MCMC 0.0, 0.0e and 0.0h (Medians are shown as horizontal lines). Dots are observed mean CSLF and vertical lines are 95% confidence intervals.

APPENDIX A: SUMMARY OF RESULTS FOR MPD IMODEL RUNS

Table A1: Description of model components for initial model runs

	Growth Model	CPUE (CV)	CPUE2 (CV)	Shape Parameter	Tag weighted	M Prior	Other
i_0.0	Exp	0.1	0.08	1	No	LN(0.1,0.1)	
i_0.0a	Exp	0.1	0.08	1	Yes	LN(0.1,0.1)	
i_0.0b	Exp	0.1	0.08	1	No	LN(0.15,0.1)	
i_0.0j	Exp	0.1	0.08	1	No	LN(0.1,0.15)	
i_0.0c	Exp	0.1	0.08	1	No	LN(0.1,0.1)	Include RDLF 1992
i_0.0d	Exp	0.1	0.08	1	No	LN(0.1,0.1)	removed tag-recapture data < 90 mm
i_0.0e	Exp	0.2	0.16	1	No	LN(0.1,0.1)	
i_0.0f	Exp	0.1	0.08	1	No	LN(0.1,0.1)	Alternative recreational catch history
i_0.0g	Exp	0.1	0.08	1	No	LN(0.1,0.1)	Combined CPUE series
i_0.0ha	Exp	0.1	0.08	0.3	No	LN(0.1,0.1)	Shape parameter estimated
i_0.0h	Exp	0.1	0.08	0.5	No	LN(0.1,0.1)	Shape parameter fixed
i_0.0i	Exp	0.1	0.08	1	No	LN(0.1,0.1)	Domed shaped fishing selectivity
i_0.0ia	Exp	0.1	0.08	1	Yes	LN(0.1,0.1)	
i_0.1	Inv	0.1	0.08	1	No	LN(0.1,0.1)	
i_0.1a	Inv	0.1	0.08	1	No	LN(0.1,0.1)	
i_0.1b	Inv	0.1	0.08	1	No	LN(0.15,0.1)	
i_0.1c	Inv	0.1	0.08	1	No	LN(0.1,0.1)	Include RDLF 1992

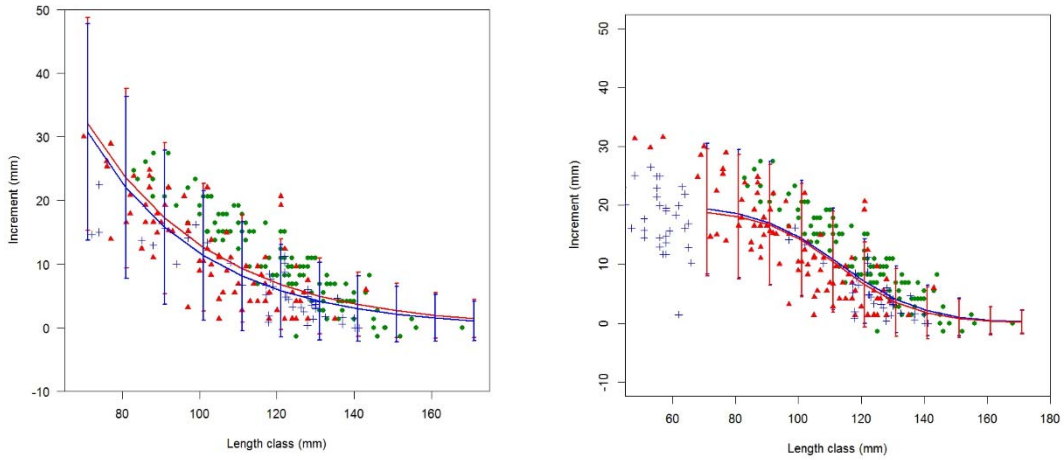

Figure A1: Expected growth model with data, left panel is the exponential growth model and the right panel is the fit using the inverse-logistic growth model. Red line is the tag data unweighted, blue line is tag data weighted by the catch.

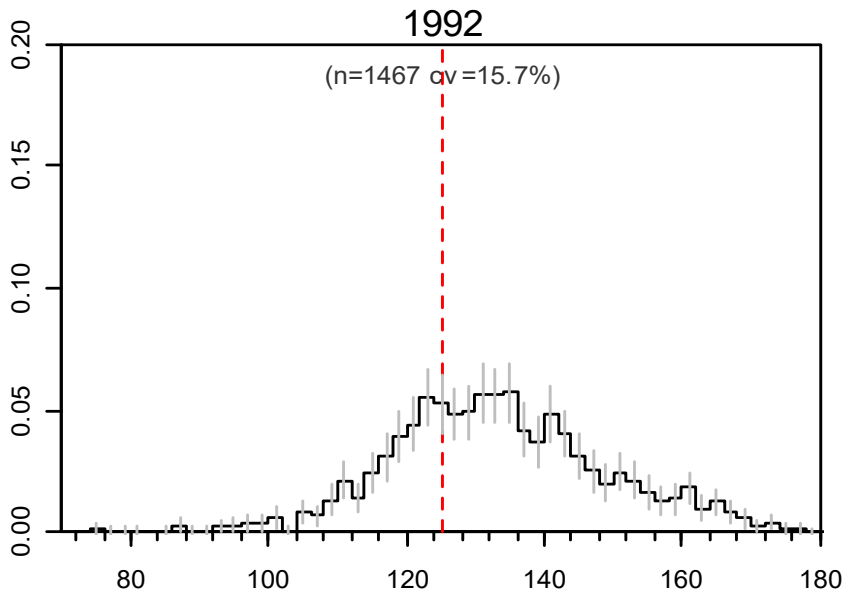

Figure A2: RDLF from 1992, showing a shoulder at the right (160 mm).

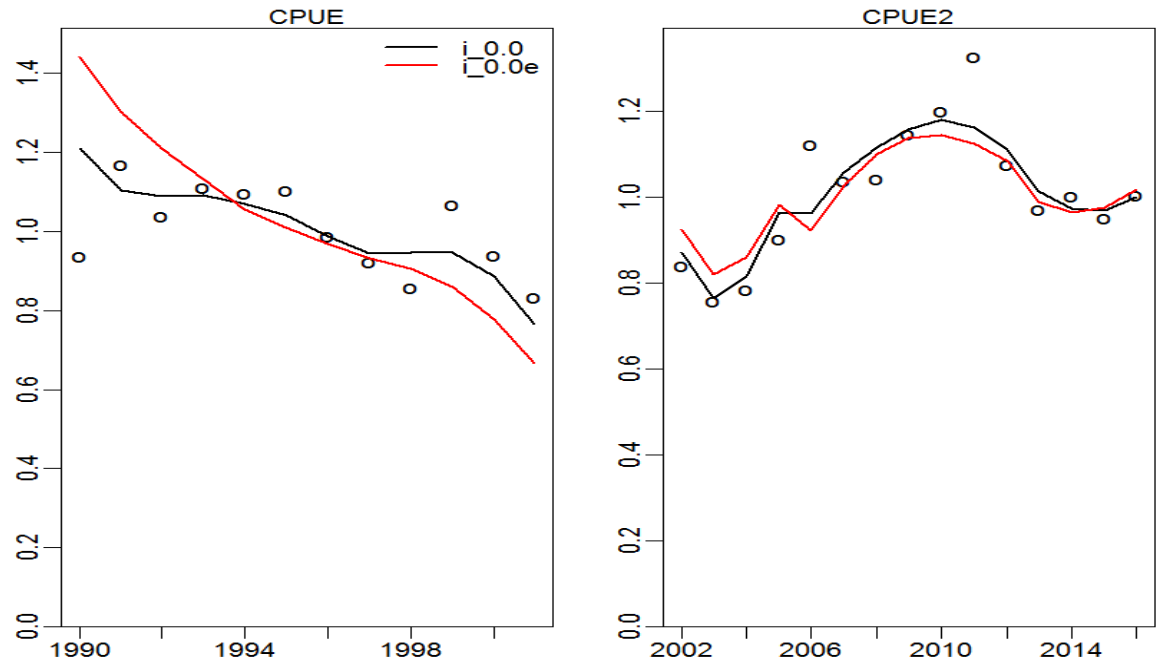

Figure A3: Comparison in fits to CPUE between base case and a preliminary model run where CV on both CPUE series was doubled.

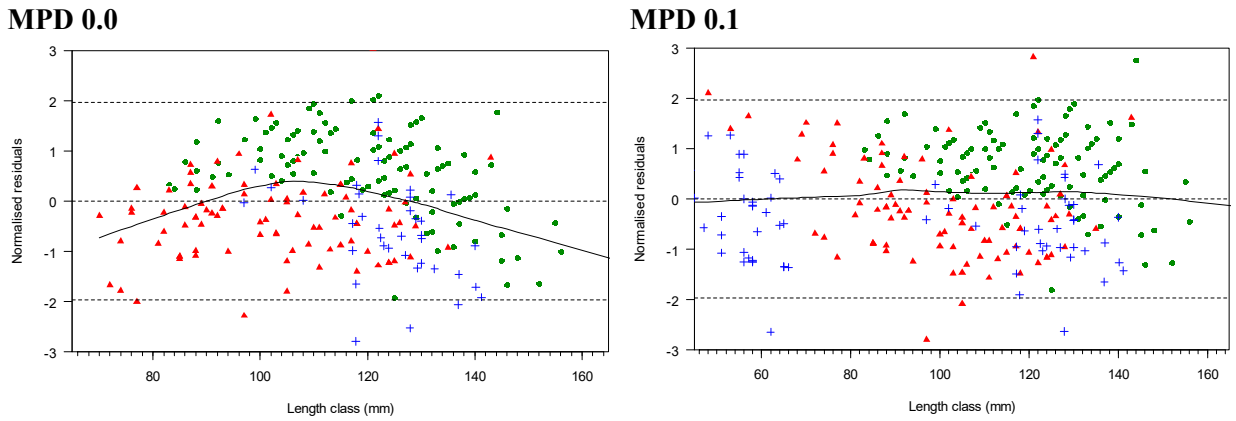

Figure A4: Normalised residuals from the fit using the exponential growth model (left panel) and the inverse-logistic growth model (right panel) to the tag recapture data. Green dots, Catlins west; red triangles, Catlins east; blue crosses, east coast. For MPD 0.1, observations with initial length less than 70 mm were also included in the model.

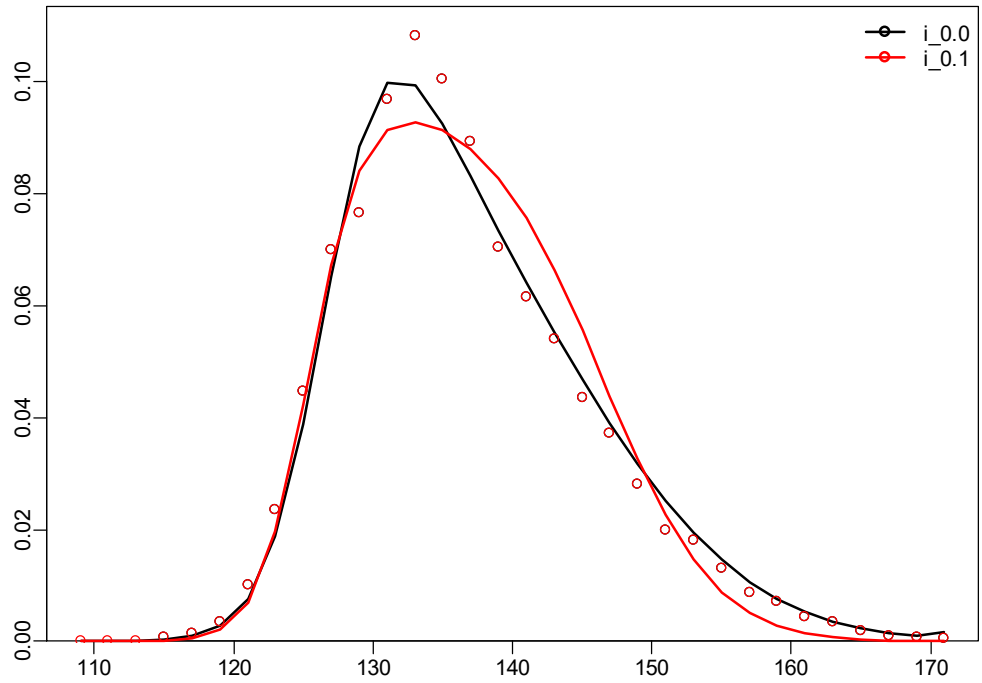

Figure A5: Comparison of fits to CSLF data averaged over all years when growth is modelled using the exponential form (black line) and inverse-logistic form (red line).

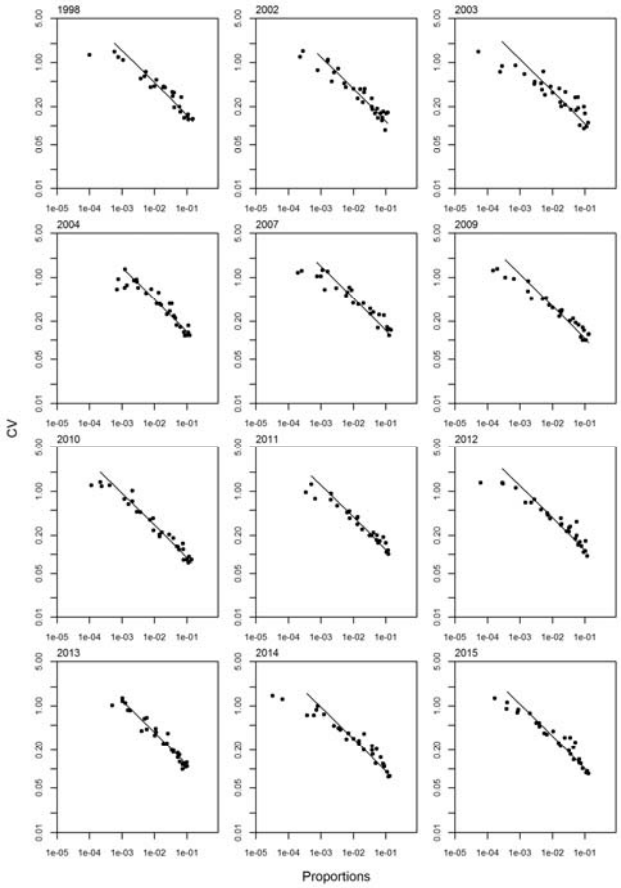

Figure A6: Estimated proportions versus CVs for the commercial catch length frequencies for PAU 5D. Lines indicate the best least squares fit for the effective sample size of the multinomial distribution.

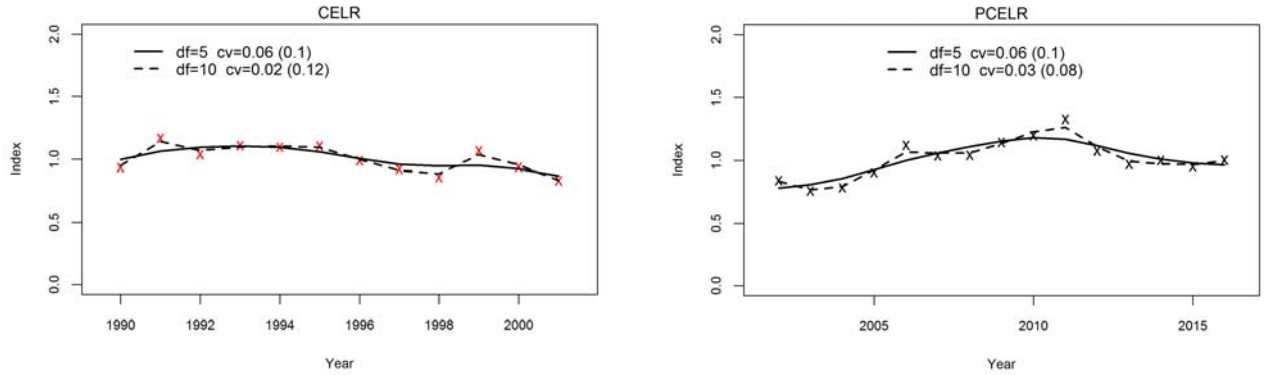

Figure A7: A series of lowess lines of various degrees of freedom (f) fitted to the PAU 5D standardised CPUE indices for 1990–2001 (left) and for 2002–2016 (right). CVs are calculated from residuals for each of the fitted lowess line and are further adjusted for the degree of "smoothing" (adjusted value in the bracket). The CV of from the "appropriate" fit will be used as the CV in the stock assessment model. What is "appropriate" is judged by visual examination of lines with different degrees of smoothing.

APPENDIX B: SUMMARY OF PROJECTIONS FOR MCMC 0.0, 0.0e AND 0.0h.

Table B1: Model 0.0 under Current TACC.

	2016	2017	2018	2019
B_t	852 (658–1157)	868 (651–1200)	872 (634–1227)	877 (613–1250)
$\%B_0$	0.35 (0.27–0.45)	0.35 (0.27–0.47)	0.36 (0.26–0.48)	0.36 (0.25–0.49)
$\%B_{msy}$	1.21 (0.95–1.58)	1.24 (0.93–1.65)	1.25 (0.91–1.69)	1.25 (0.88–1.73)
rB_t	529 (386–758)	540 (384–780)	541 (377–792)	544 (366–814)
$\%rB_0$	0.26 (0.19–0.35)	0.26 (0.19–0.36)	0.26 (0.19–0.37)	0.27 (0.18–0.38)
$\%rB_{msy}$	1.40 (0.97–2.12)	1.42 (0.97–2.19)	1.42 (0.94–2.20)	1.43 (0.91–2.25)
Pr (>Bmsy)	0.94	0.94	0.92	0.90
Pr (>Bcurrent)	0.00	0.58	0.56	0.56
Pr (>40%B0)	0.14	0.20	0.23	0.26
Pr (<20%B0)	0.00	0.00	0.00	0.00
Pr (<10%B0)	0.00	0.00	0.00	0.00
Pr (>rBmsy)	0.96	0.96	0.96	0.95
Pr (>rBcurrent)	0.00	0.78	0.65	0.59
Pr (U>U40%B0)	0.32	0.71	0.71	0.70

Table B2: Model 0.0 under 20% TACC reduction.

	2016	2017	2018	2019
B_t	852 (658–1157)	877 (660–1209)	898 (661–1253)	920 (658–1293)
$\%B_0$	0.35 (0.28–0.45)	0.36 (0.27–0.47)	0.37 (0.27–0.50)	0.38 (0.27–0.51)
$\%B_{msy}$	1.21 (0.95–1.58)	1.25 (0.95–1.66)	1.28 (0.94–1.73)	1.31 (0.94–1.79)
rB_t	529 (386–758)	549 (393–788)	567 (404–818)	587 (410–856)
$\%rB_0$	0.26 (0.19–0.35)	0.27 (0.20–0.37)	0.28 (0.20–0.38)	0.29 (0.20–0.40)
$\%rB_{msy}$	1.40 (0.97–2.12)	1.44 (0.99–2.21)	1.5 (1.0–2.3)	1.5 (1.0–2.4)
Pr (>Bmsy)	0.94	0.95	0.95	0.95
Pr (>Bcurrent)	0.00	0.66	0.72	0.75
Pr (>40%B0)	0.14	0.21	0.29	0.35
Pr (<20%B0)	0.00	0.00	0.00	0.00
Pr (<10%B0)	0.00	0.00	0.00	0.00
Pr (>rBmsy)	0.96	0.97	0.98	0.98
Pr (>rBcurrent)	0.00	0.95	0.96	0.93
Pr (U>U40%B0)	0.32	0.42	0.37	0.32

Table B3: Model 0.0 under 30% TACC reduction.

	2016	2017	2018	2019
B_t	852 (658–1157)	881 (664–1213)	912 (674–1266)	942 (680–1315)
$\%B_0$	0.35 (0.27–0.45)	0.36 (0.27–0.48)	0.37 (0.28–0.50)	0.38 (0.28–0.52)
$\%B_{msy}$	1.21 (0.95–1.58)	1.26 (0.95–1.67)	1.30 (0.96–1.75)	1.34 (0.97–1.82)
rB_t	529 (386–758)	554 (398–793)	580 (417–831)	608 (432–877)
$\%rB_0$	0.26 (0.19–0.35)	0.27 (0.20–0.37)	0.28 (0.21–0.39)	0.30 (0.21–0.41)
$\%rB_{msy}$	1.40 (0.97–2.12)	1.5 (1.0–2.2)	1.5 (1.0–2.3)	1.6 (1.1–2.4)
Pr (>Bmsy)	0.94	0.95	0.96	0.96
Pr (>Bcurrent)	0.00	0.70	0.79	0.83
Pr (>40%B0)	0.14	0.23	0.32	0.40
Pr (<20%B0)	0.00	0.00	0.00	0.00
Pr (<10%B0)	0.00	0.00	0.00	0.00
Pr (>rBmsy)	0.96	0.98	0.99	0.99
Pr (>rBcurrent)	0.00	0.99	0.99	0.99
Pr (U>U40%B0)	0.32	0.26	0.20	0.14

Table B4: Model 0.0 under 50% TACC reduction.

	2016	2017	2018	2019
B_t	852 (658–1157)	890 (674–1222)	938 (701–1292)	986 (724–1358)
$\%B_0$	0.35 (0.27–0.45)	0.36 (0.28–0.48)	0.38 (0.29–0.51)	0.40 (0.30–0.54)
$\%B_{msy}$	1.21 (0.95–1.58)	1.27 (0.97–1.68)	1.3 (1.0–1.8)	1.4 (1.0–1.9)
rB_t	529 (386–758)	563 (407–802)	606 (444–858)	651 (475–919)
$\%rB_0$	0.26 (0.19–0.35)	0.27 (0.20–0.37)	0.30 (0.22–0.40)	0.32 (0.23–0.43)
$\%rB_{msy}$	1.40 (0.97–2.12)	1.5 (1.0–2.2)	1.6 (1.1–2.4)	1.7 (1.2–2.6)
Pr (>Bmsy)	0.94	0.96	0.98	0.99
Pr (>Bcurrent)	0.00	0.78	0.90	0.94
Pr (>40%B0)	0.14	0.25	0.38	0.51
Pr (<20%B0)	0.00	0.00	0.00	0.00
Pr (<10%B0)	0.00	0.00	0.00	0.00
Pr (>rBmsy)	0.96	0.98	0.99	1.00
Pr (>rBcurrent)	0.00	1.00	1.00	1.00
Pr (U>U40%B0)	0.32	0.04	0.01	0.01

Table 6: Model 0.0 under 50% TACC reduction with recreational catch = 20 t.

	2016	2017	2018	2019
B_t	852 (658–1157)	885 (668–1217)	923 (686–1277)	961 (700–1334)
$\%B_0$	0.35 (0.27–0.45)	0.36 (0.28–0.48)	0.38 (0.28–0.51)	0.39 (0.29–0.53)
$\%B_{msy}$	1.21 (0.95–1.58)	1.26 (0.96–1.67)	1.32 (0.98–1.76)	1.4 (1.0–1.8)
rB_t	529 (386–758)	558 (402–797)	592 (429–843)	627 (451–895)
$\%rB_0$	0.26 (0.19–0.35)	0.27 (0.20–0.37)	0.29 (0.21–0.39)	0.31 (0.22–0.42)
$\%rB_{msy}$	1.40 (0.97–2.12)	1.5 (1.0–2.2)	1.6 (1.1–2.3)	1.7 (1.1–2.5)
Pr (>Bmsy)	0.94	0.96	0.97	0.97
Pr (>Bcurrent)	0.00	0.74	0.84	0.89
Pr (>40%B0)	0.14	0.23	0.34	0.45
Pr (<20%B0)	0.00	0.00	0.00	0.00
Pr (<10%B0)	0.00	0.00	0.00	0.00
Pr (>rBmsy)	0.96	0.98	0.99	0.99
Pr (>rBcurrent)	0.00	1.00	1.00	1.00
Pr (U>U40%B0)	0.32	0.14	0.08	0.04

Table B6: Model 0.0e under Current TACC.

	2016	2017	2018	2019
B_t	811 (596–1167)	830 (590–1210)	836 (572–1239)	843 (551–1272)
$\%B_0$	0.31 (0.23–0.43)	0.32 (0.23–0.45)	0.32 (0.22–0.46)	0.33 (0.21–0.48)
$\%B_{msy}$	1.1 (0.8–1.5)	1.1 (0.8–1.6)	1.12 (0.77–1.62)	1.13 (0.74–1.67)
rB_t	514 (351–789)	525 (346–820)	525 (336–829)	528 (326–844)
$\%rB_0$	0.23 (0.16–0.34)	0.24 (0.16–0.36)	0.24 (0.15–0.36)	0.24 (0.15–0.37)
$\%rB_{msy}$	1.16 (0.75–1.89)	1.18 (0.74–1.95)	1.19 (0.72–1.98)	1.2 (0.7–2.0)
Pr (>Bmsy)	0.70	0.73	0.73	0.73
Pr (>Bcurrent)	0.00	0.62	0.60	0.60
Pr (>40%B0)	0.07	0.10	0.12	0.14
Pr (<20%B0)	0.00	0.00	0.01	0.01
Pr (<10%B0)	0.00	0.00	0.00	0.00
Pr (>rBmsy)	0.74	0.76	0.75	0.74
Pr (>rBcurrent)	0.00	0.78	0.66	0.61
Pr (U>U40%B0)	0.65	0.88	0.87	0.86

Table B7: Model 0.0e under 20% TACC reduction.

	2016	2017	2018	2019
B_t	811 (596–1167)	839 (599–1219)	863 (599–1265)	887 (596–1316)
$\%B_0$	0.31 (0.23–0.43)	0.32 (0.23–0.45)	0.33 (0.23–0.47)	0.34 (0.23–0.49)
$\%B_{msy}$	1.1 (0.8–1.5)	1.13 (0.81–1.58)	1.2 (0.8–1.7)	1.2 (0.8–1.7)
rB_t	514 (351–789)	534 (355–829)	552 (363–856)	572 (371–886)
$\%rB_0$	0.23 (0.16–0.34)	0.24 (0.16–0.36)	0.25 (0.16–0.37)	0.26 (0.17–0.39)
$\%rB_{msy}$	1.16 (0.75–1.89)	1.20 (0.76–1.97)	1.25 (0.77–2.04)	1.30 (0.79–2.11)
Pr (>Bmsy)	0.70	0.75	0.79	0.81
Pr (>Bcurrent)	0.00	0.71	0.76	0.79
Pr (>40%B0)	0.07	0.11	0.15	0.20
Pr (<20%B0)	0.00	0.00	0.00	0.00
Pr (<10%B0)	0.00	0.00	0.00	0.00
Pr (>rBmsy)	0.74	0.78	0.82	0.85
Pr (>rBcurrent)	0.00	0.95	0.96	0.93
Pr (U>U40%B0)	0.65	0.71	0.66	0.61

Table 7: Model 0.0e under 30% TACC reduction.

Year	2016	2017	2018	2019
B_t	811 (596–1167)	844 (603–1224)	876 (613–1278)	910 (618–1338)
$\%B_0$	0.31 (0.23–0.43)	0.33 (0.23–0.45)	0.34 (0.24–0.48)	0.35 (0.24–0.50)
$\%B_{msy}$	1.1 (0.8–1.5)	1.14 (0.81–1.59)	1.18 (0.82–1.68)	1.22 (0.83–1.76)
rB_t	514 (351–789)	538 (360–833)	565 (377–869)	593 (393–908)
$\%rB_0$	0.23 (0.16–0.34)	0.24 (0.16–0.36)	0.25 (0.17–0.38)	0.27 (0.18–0.40)
$\%rB_{msy}$	1.16 (0.75–1.89)	1.21 (0.77–1.98)	1.3 (0.8–2.1)	1.35 (0.84–2.17)
Pr (>Bmsy)	0.70	0.77	0.81	0.85
Pr (>Bcurrent)	0.00	0.75	0.83	0.87
Pr (>40%B0)	0.07	0.11	0.17	0.23
Pr (<20%B0)	0.00	0.00	0.00	0.00
Pr (<10%B0)	0.00	0.00	0.00	0.00
Pr (>rBmsy)	0.74	0.80	0.85	0.89
Pr (>rBcurrent)	0.00	0.98	0.99	0.99
Pr (U>U40%B0)	0.65	0.57	0.50	0.42

Table B9: Model 0.0e under 50% TACC reduction.

	2016	2017	2018	2019
B_t	811 (596–1167)	853 (613–1232)	903 (640–1305)	954 (663–1381)
$\%B_0$	0.31 (0.23–0.43)	0.33 (0.24–0.46)	0.35 (0.25–0.49)	0.37 (0.26–0.52)
$\%B_{msy}$	1.1 (0.8–1.5)	1.15 (0.83–1.60)	1.22 (0.86–1.71)	1.28 (0.89–1.82)
rB_t	514 (351–789)	547 (369–842)	592 (403–896)	637 (437–951)
$\%rB_0$	0.23 (0.16–0.34)	0.25 (0.17–0.37)	0.27 (0.18–0.39)	0.29 (0.20–0.42)
$\%rB_{msy}$	1.16 (0.75–1.89)	1.23 (0.79–2.00)	1.34 (0.86–2.13)	1.44 (0.93–2.28)
Pr (>Bmsy)	0.70	0.79	0.87	0.91
Pr (>Bcurrent)	0.00	0.83	0.93	0.97
Pr (>40%B0)	0.07	0.13	0.20	0.30
Pr (<20%B0)	0.00	0.00	0.00	0.00
Pr (<10%B0)	0.00	0.00	0.00	0.00
Pr (>rBmsy)	0.74	0.82	0.90	0.95
Pr (>rBcurrent)	0.00	1.00	1.00	1.00
Pr (U>U40%B0)	0.65	0.24	0.15	0.08

Table B10: Model 0.0e under 50% TACC reduction with recreational catch = 20 t.

	2016	2017	2018	2019
B_t	811 (596–1167)	848 (607–1227)	888 (625–1290)	929 (638–1357)
$\%B_0$	0.31 (0.23–0.43)	0.33 (0.24–0.46)	0.34 (0.24–0.48)	0.36 (0.25–0.51)
$\%B_{msy}$	1.1 (0.8–1.5)	1.14 (0.82–1.60)	1.19 (0.84–1.69)	1.25 (0.86–1.78)
rB_t	514 (351–789)	542 (364–837)	577 (388–881)	612 (413–927)
$\%rB_0$	0.23 (0.16–0.34)	0.24 (0.16–0.36)	0.26 (0.18–0.38)	0.28 (0.19–0.41)
$\%rB_{msy}$	1.16 (0.75–1.89)	1.22 (0.78–1.99)	1.30 (0.83–2.10)	1.39 (0.87–2.22)
Pr (>Bmsy)	0.70	0.78	0.83	0.88
Pr (>Bcurrent)	0.00	0.78	0.88	0.92
Pr (>40%B0)	0.07	0.12	0.18	0.26
Pr (<20%B0)	0.00	0.00	0.00	0.00
Pr (<10%B0)	0.00	0.00	0.00	0.00
Pr (>rBmsy)	0.74	0.81	0.87	0.92
Pr (>rBcurrent)	0.00	0.99	1.00	1.00
Pr (U>U40%B0)	0.65	0.43	0.34	0.25

Table B11: Model 0.0h under Current TACC.

	2016	2017	2018	2019
B_t	713 (531–1022)	730 (521–1063)	735 (494–1096)	740 (469–1136)
$\%B_0$	0.28 (0.21–0.39)	0.29 (0.20–0.41)	0.29 (0.19–0.42)	0.29 (0.18–0.44)
$\%B_{msy}$	0.97 (0.71–1.36)	0.99 (0.70–1.42)	1.00 (0.66–1.47)	1.01 (0.63–1.53)
rB_t	433 (299–672)	440 (294–691)	438 (279–697)	443 (262–719)
$\%rB_0$	0.20 (0.13–0.30)	0.20 (0.13–0.31)	0.20 (0.13–0.31)	0.20 (0.12–0.32)
$\%rB_{msy}$	0.98 (0.63–1.60)	1.00 (0.62–1.65)	1.00 (0.58–1.69)	1.00 (0.55–1.73)
Pr (>Bmsy)	0.43	0.48	0.50	0.51
Pr (>Bcurrent)	0.00	0.58	0.56	0.56
Pr (>40%B0)	0.02	0.03	0.04	0.07
Pr (<20%B0)	0.01	0.02	0.04	0.05
Pr (<10%B0)	0.00	0.00	0.00	0.00
Pr (>rBmsy)	0.46	0.50	0.50	0.50
Pr (>rBcurrent)	0.00	0.69	0.56	0.53
Pr (U>U40%B0)	0.85	0.96	0.96	0.95

Table B12: Model 0.0h under 20% TACC reduction.

	2016	2017	2018	2019
B_t	713 (531–1022)	739 (530–1072)	762 (522–1123)	785 (515–1180)
$\%B_0$	0.28 (0.21–0.39)	0.29 (0.21–0.41)	0.30 (0.20–0.43)	0.31 (0.20–0.46)
$\%B_{msy}$	0.97 (0.71–1.36)	1.01 (0.71–1.44)	1.0 (0.7–1.5)	1.1 (0.7–1.6)
rB_t	433 (299–672)	449 (304–700)	465 (307–724)	487 (306–762)
$\%rB_0$	0.20 (0.13–0.30)	0.21 (0.14–0.31)	0.21 (0.14–0.33)	0.22 (0.14–0.34)
$\%rB_{msy}$	0.98 (0.63–1.60)	1.02 (0.63–1.68)	1.06 (0.64–1.75)	1.10 (0.65–1.84)
Pr (>Bmsy)	0.43	0.51	0.58	0.62
Pr (>Bcurrent)	0.00	0.66	0.72	0.75
Pr (>40%B0)	0.02	0.04	0.06	0.10
Pr (<20%B0)	0.01	0.01	0.02	0.02
Pr (<10%B0)	0.00	0.00	0.00	0.00
Pr (>rBmsy)	0.46	0.53	0.59	0.64
Pr (>rBcurrent)	0.00	0.91	0.93	0.89
Pr (U>U40%B0)	0.85	0.89	0.86	0.83

Table B13: Model 0.0h under 30% TACC reduction.

	2016	2017	2018	2019
B_t	713 (531–1022)	744 (535–1077)	776 (536–1136)	807 (538–1202)
$\%B_0$	0.28 (0.21–0.39)	0.29 (0.21–0.41)	0.30 (0.21–0.44)	0.32 (0.21–0.46)
$\%B_{msy}$	0.97 (0.71–1.36)	1.01 (0.72–1.44)	1.06 (0.72–1.53)	1.10 (0.73–1.62)
rB_t	433 (299–672)	454 (308–705)	479 (320–737)	508 (328–784)
$\%rB_0$	0.20 (0.13–0.30)	0.21 (0.14–0.31)	0.22 (0.14–0.33)	0.23 (0.15–0.35)
$\%rB_{msy}$	0.98 (0.63–1.60)	1.03 (0.64–1.69)	1.09 (0.67–1.79)	1.15 (0.69–1.89)
Pr (>Bmsy)	0.43	0.53	0.61	0.68
Pr (>Bcurrent)	0.00	0.70	0.79	0.83
Pr (>40%B0)	0.02	0.04	0.07	0.12
Pr (<20%B0)	0.01	0.01	0.01	0.01
Pr (<10%B0)	0.00	0.00	0.00	0.00
Pr (>rBmsy)	0.46	0.55	0.64	0.71
Pr (>rBcurrent)	0.00	0.97	0.99	0.98
Pr (U>U40%B0)	0.85	0.81	0.75	0.68

Table B14: Model 0.0h under 50% TACC reduction.

	2016	2017	2018	2019
B_t	713 (531–1022)	753 (544–1086)	803 (563–1163)	852 (583–1245)
$\%B_0$	0.28 (0.21–0.39)	0.30 (0.21–0.42)	0.32 (0.22–0.45)	0.33 (0.23–0.48)
$\%B_{msy}$	0.97 (0.71–1.36)	1.02 (0.73–1.45)	1.09 (0.76–1.56)	1.16 (0.79–1.69)
rB_t	433 (299–672)	463 (317–714)	505 (348–764)	552 (373–828)
$\%rB_0$	0.20 (0.13–0.30)	0.21 (0.14–0.32)	0.23 (0.16–0.34)	0.25 (0.17–0.37)
$\%rB_{msy}$	0.98 (0.63–1.60)	1.05 (0.66–1.71)	1.15 (0.73–1.85)	1.25 (0.78–1.99)
Pr (>Bmsy)	0.43	0.56	0.69	0.78
Pr (>Bcurrent)	0.00	0.79	0.91	0.95
Pr (>40%B0)	0.02	0.04	0.09	0.17
Pr (<20%B0)	0.01	0.01	0.01	0.00
Pr (<10%B0)	0.00	0.00	0.00	0.00
Pr (>rBmsy)	0.46	0.58	0.73	0.83
Pr (>rBcurrent)	0.00	1.00	1.00	1.00
Pr (U>U40%B0)	0.85	0.51	0.36	0.23

Table B15: Model 0.0h under 50% TACC reduction with recreational catch = 20 t.

	2016	2017	2018	2019
B_t	713 (531–1022)	748 (539–1080)	788 (548–1148)	827 (558–1221)
$\%B_0$	0.28 (0.21–0.39)	0.29 (0.21–0.41)	0.31 (0.21–0.44)	0.32 (0.22–0.47)
$\%B_{msy}$	0.97 (0.71–1.36)	1.02 (0.73–1.45)	1.07 (0.74–1.55)	1.13 (0.76–1.65)
rB_t	433 (299–672)	458 (312–709)	490 (332–749)	527 (348–803)
$\%rB_0$	0.20 (0.13–0.30)	0.21 (0.14–0.32)	0.22 (0.15–0.34)	0.24 (0.16–0.36)
$\%rB_{msy}$	0.98 (0.63–1.60)	1.04 (0.65–1.70)	1.1 (0.7–1.8)	1.19 (0.73–1.93)
Pr (>Bmsy)	0.43	0.54	0.65	0.72
Pr (>Bcurrent)	0.00	0.74	0.85	0.90
Pr (>40%B0)	0.02	0.04	0.08	0.14
Pr (<20%B0)	0.01	0.01	0.01	0.01
Pr (<10%B0)	0.00	0.00	0.00	0.00
Pr (>rBmsy)	0.46	0.56	0.68	0.77
Pr (>rBcurrent)	0.00	0.99	1.00	1.00
Pr (U>U40%B0)	0.85	0.70	0.61	0.50

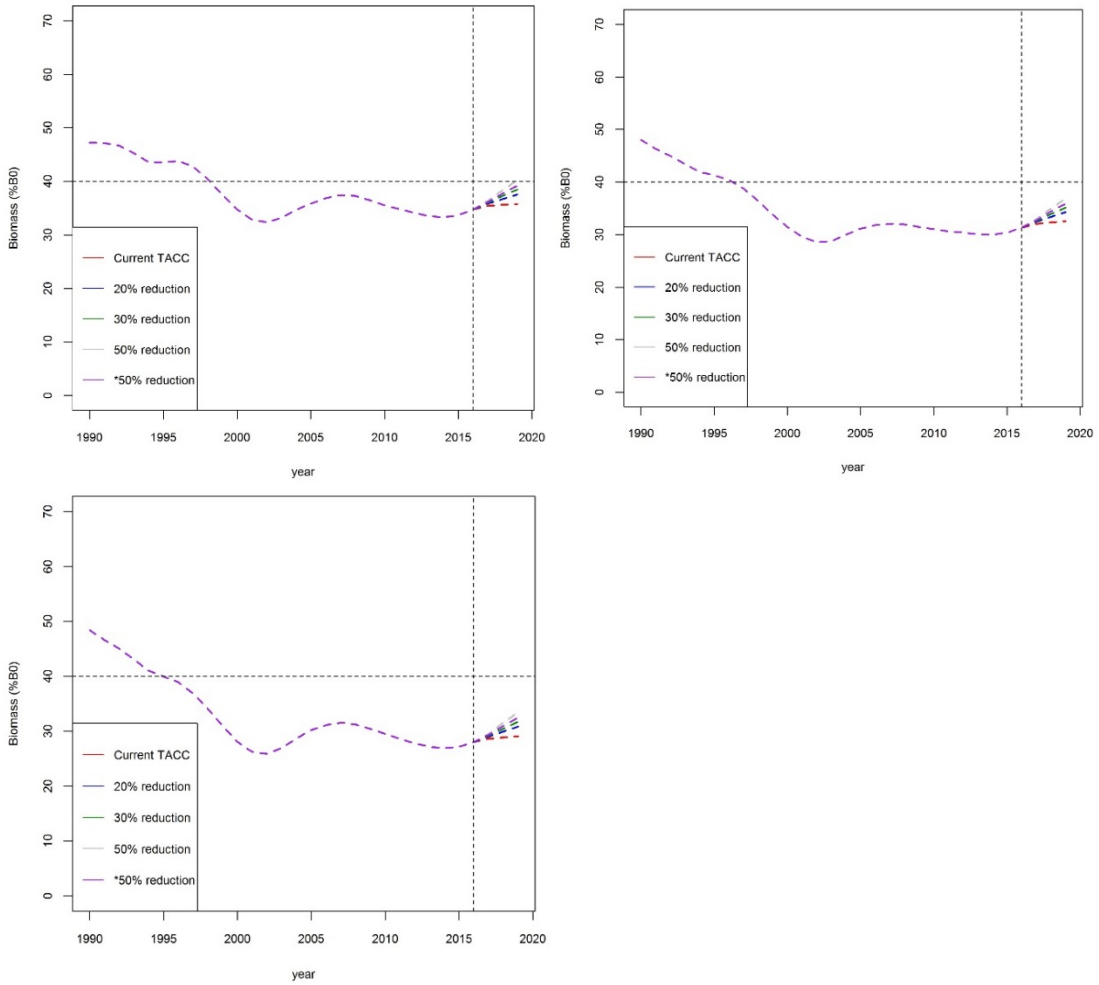

Figure B1: Median projected biomass under five sets of future catch scenarios, top left is the base case model 0.0, top right is the model 0.0e and bottom left is model 0.0h.

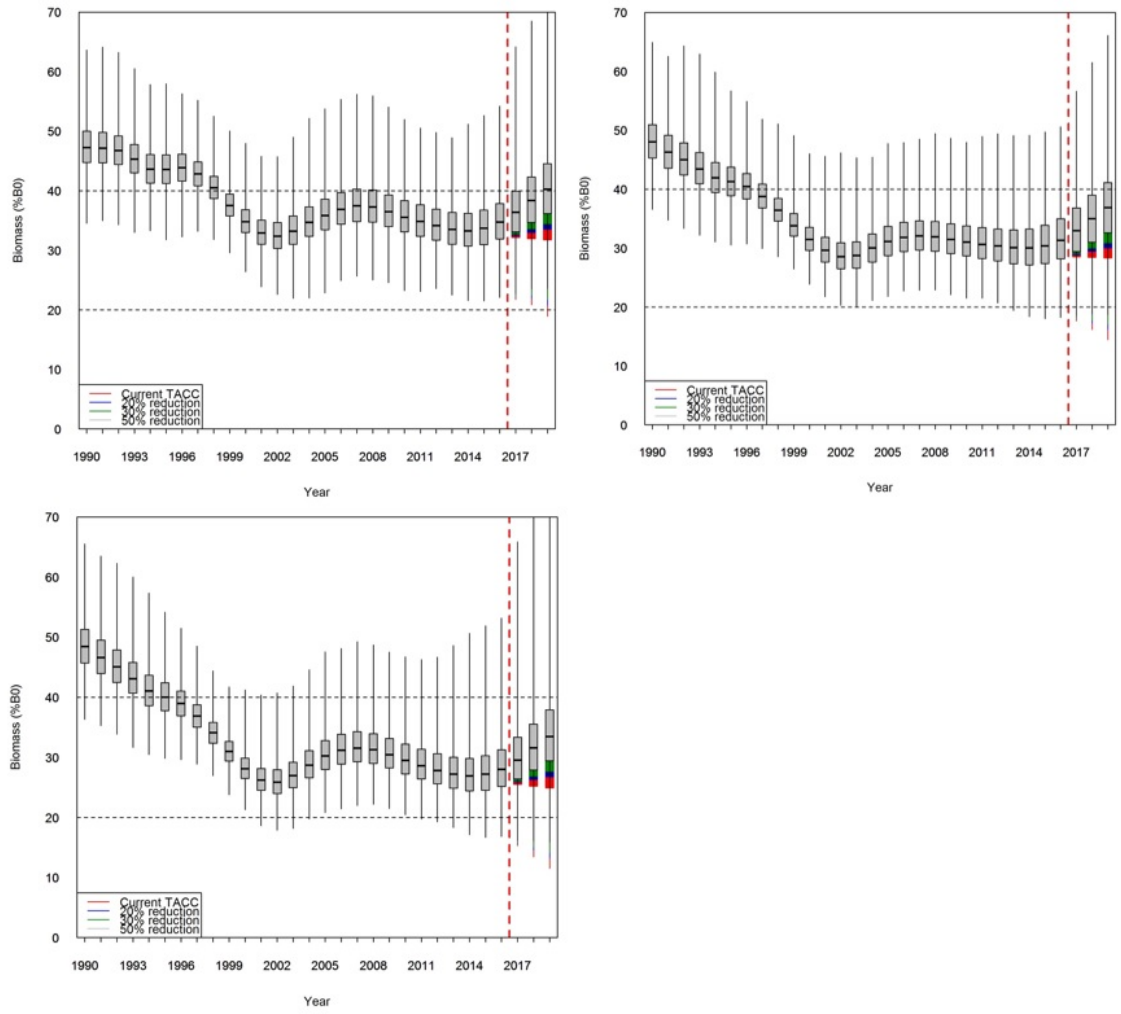

Figure B2: Projected biomass under five sets of future catch scenarios. Top left is the base case model 0.0, top right is the model 0.0e and bottom left is model 0.0h. Box represents 25% and 50% quantiles while the whiskers show the full distribution.

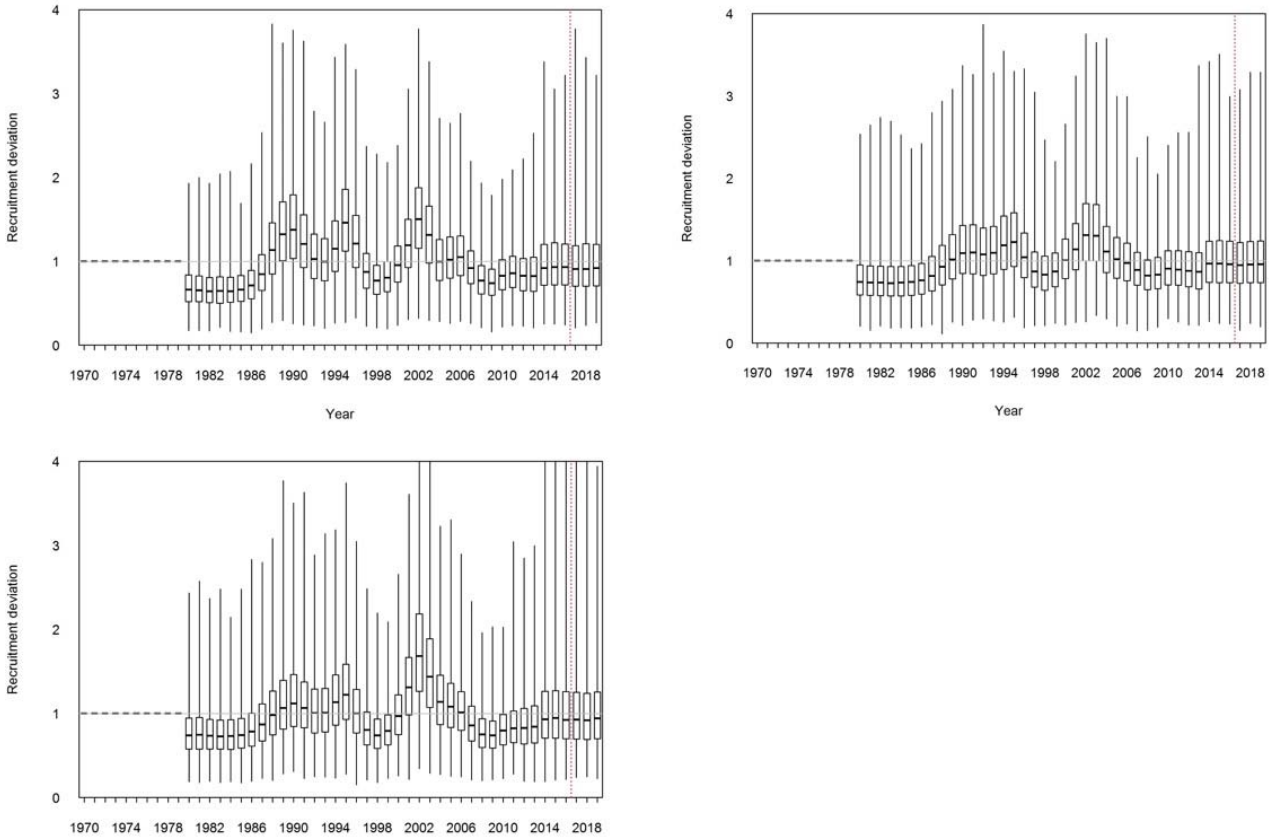

Figure B3: Randomised recruitment used for the projections, where recruitment for 2002–2012 were resampled. Top left is the base case model 0.0, top right is the model 0.0e and bottom left is model 0.0h.